Journal of Medicinal Chemistry

pubs.acs.org/jmc

Article

D-*chiro*-Inositol Ribophostin: A Highly Potent Agonist of D-*myo*-Inositol 1,4,5-Trisphosphate Receptors: Synthesis and Biological Activities

Stephen J. Mills, Ana M. Rossi, Vera Konieczny, Daniel Bakowski, Colin W. Taylor, and Barry V. L. Potter*

Cite This: *J. Med. Chem.* 2020, 63, 3238−3251

Read Online

ACCESS | Metrics & More | Article Recommendations | Supporting Information

ABSTRACT: Analogues of the Ca^{2+}-releasing intracellular messenger D-*myo*-inositol 1,4,5-trisphosphate [**1**, Ins(1,4,5)P_3] are important synthetic targets. Replacement of the α-glucopyranosyl motif in the natural product mimic adenophostin **2** by D-*chiro*-inositol in D-*chiro*-inositol adenophostin **4** increased the potency. Similar modification of the non-nucleotide Ins(1,4,5)P_3 mimic ribophostin **6** may increase the activity. D-*chiro*-Inositol ribophostin **10** was synthesized by coupling as building blocks suitably protected ribose **12** with L-(+)-3-*O*-trifluoromethylsulfonyl-6-*O*-*p*-methoxybenzyl-1,2:4,5-di-*O*-isopropylidene-*myo*-inositol **11**. Separable diastereoisomeric 3-*O*-camphanate esters of (±)-6-*O*-*p*-methoxy-benzyl-1,2:4,5-di-*O*-isopropylidene-*myo*-inositol allowed the preparation of **11**. Selective *trans*-isopropylidene deprotection in coupled **13**, then monobenzylation gave separable regioisomers **15** and **16**. *p*-Methoxybenzyl group deprotection of **16**, phosphitylation/oxidation, then deprotection afforded **10**, which was a full agonist in Ca^{2+}-release assays; its potency and binding affinity for Ins(1,4,5)P_3R were similar to those of adenophostin. Both **4** and **10** elicited a store-operated Ca^{2+} current I_{CRAC} in patch-clamped cells, unlike Ins(1,4,5)P_3 consistent with resistance to metabolism. D-*chiro*-Inositol ribophostin is the most potent small-molecule Ins(1,4,5)P_3 receptor agonist without a nucleobase yet synthesized.

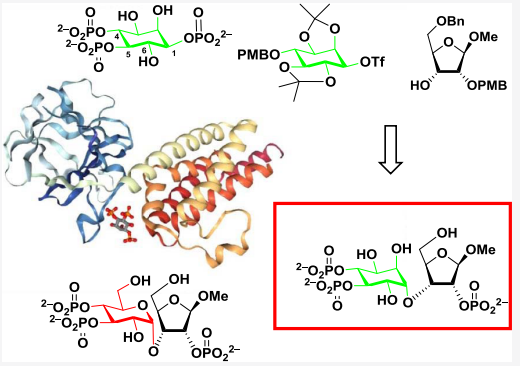

INTRODUCTION

Phospholipase C hydrolyzes phosphatidylinositol 4,5-bisphosphate to release the water-soluble second messenger, D-*myo*-inositol 1,4,5-trisphosphate [Ins(1,4,5)P_3 **1**, Figure 1]. Ins(1,4,5)P_3 binds to the Ins(1,4,5)P_3-binding core (IBC) of its receptor (Ins(1,4,5)P_3R),[1] a tetrameric structure with an intrinsic Ca^{2+}-permeable pore that opens after Ins(1,4,5)P_3 binding.[2−4] This allows Ca^{2+} to be released from intracellular stores to the cytosol to cause an increase in cytosolic Ca^{2+} concentration. Hence, Ins(1,4,5)P_3 links the many extracellular stimuli that activate phospholipase C to the Ca^{2+} signals that regulate diverse activities in animal cells. We have previously synthesized numerous modified ligands to probe their interactions with Ins(1,4,5)P_3Rs.[5−7] Such ligands include modifications or mimics of Ins(1,4,5)P_3 and also simplified benzene polyphosphate surrogates.[6,7]

The natural product glyconucleotides adenophostin A **2** and adenophostin B **3** (Figure 1) were isolated from fungal broths[8−10] and shown to be ca. 10-fold more potent than Ins(1,4,5)P_3 in evoking Ca^{2+} release through each of the three mammalian Ins(1,4,5)P_3R subtypes (Ins(1,4,5)P_3R1−3).[11]

D-*myo*-Inositol 1,4,5-trisphosphate **1** (Ins(1,4,5)P_3)

R = H Adenophostin A (**2**)
R = Ac Adenophostin B (**3**)

D-*chiro*-Inositol Adenophostin (**4**)

Figure 1. Structures of inositol trisphosphate **1**, the adenophostins **2** and **3**, and inositol adenophostin **4**.

Received: November 29, 2019
Published: February 13, 2020

https://dx.doi.org/10.1021/acs.jmedchem.9b01986
J. Med. Chem. 2020, 63, 3238−3251

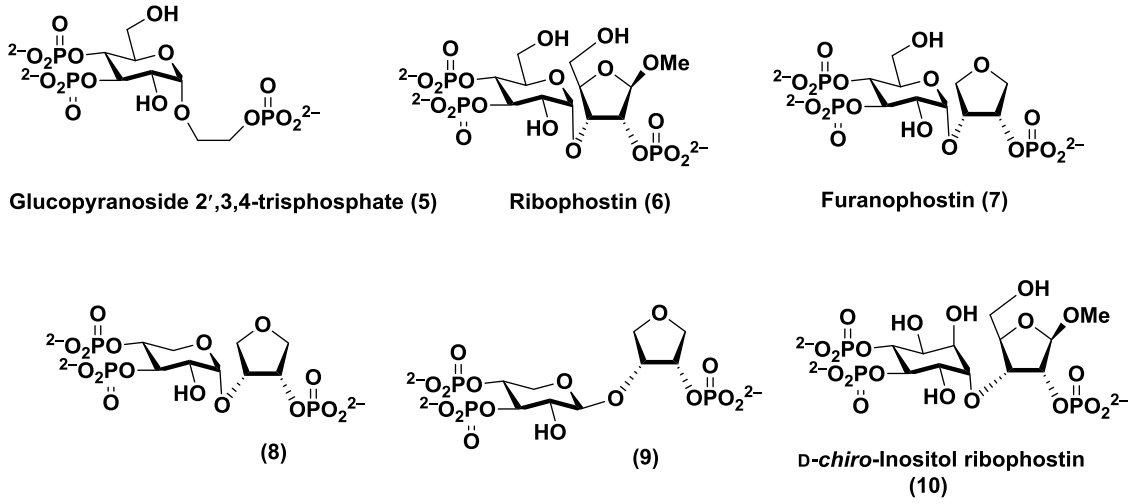

Figure 2. Structures of synthetic Ins(1,4,5)P_3 mimics based on part of adenophostin, including ribophostin **6** and inositol ribophostin **10**.

Scheme 1. Coupling of the Suitably Protected Inositol Triflate 11 and Ribose 12 Building Blocks, Selective Deprotection, and Benzylation To Give the Separable Regioisomers 15 and 16 and Selective Deprotection of 16 To Afford Intermediate 17 for Phosphorylation

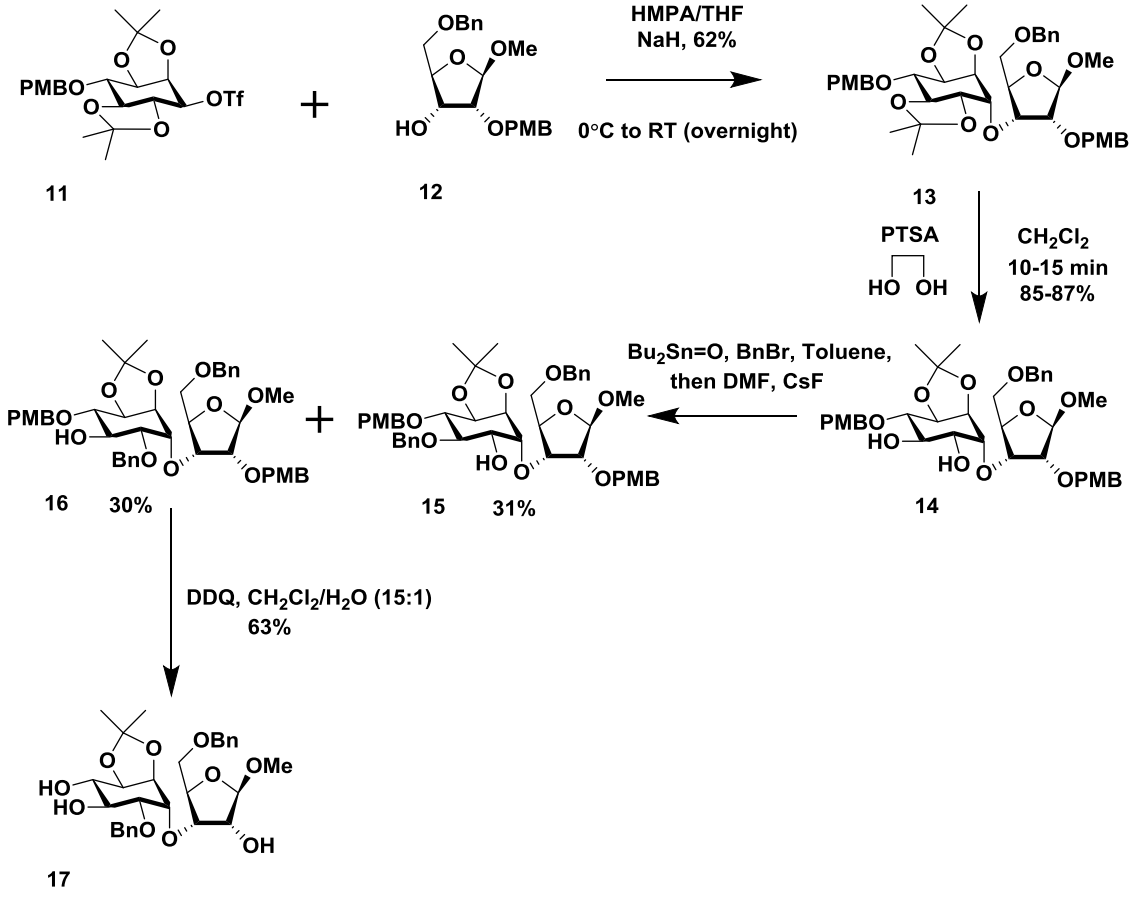

Their structure has inspired much synthetic work by us[11−13] and others[14−17] and provided numerous ligands with modifications at the phosphate groups, nucleobase motif, and at both sugars.[11,18,19] However, the bisphosphorylated glucose moiety that is thought to mimic the key Ins(1,4,5)P_3 pharmacophore has never been replaced by a cyclitol bisphosphate structure until very recently.[20] Here, the glucose motif of adenophostin A was replaced with D-*chiro*-inositol[20] and thus the pyranose−furanose disaccharide linkage was replaced with a *sec*−*sec* ether to give D-*chiro*-inositol adenophostin **4**, which is nearly 2-fold more potent than adenophostin A.[20]

Our model for the interaction of adenophostin A with the Ins(1,4,5)P_3 binding core (IBC; residues 224−604 in Ins(1,4,5)P_3R1)[21] is supported by mutagenesis[22] and SAR analyses[13,19,23−25] and suggests that the glucose 3″,4″-

https://dx.doi.org/10.1021/acs.jmedchem.9b01986
J. Med. Chem. 2020, 63, 3238−3251

Scheme 2. Phosphitylation of 17, Oxidation of Resulting 18 to 19, and Complete Deprotection of 19 To Give the Target Inositol Ribophostin 10

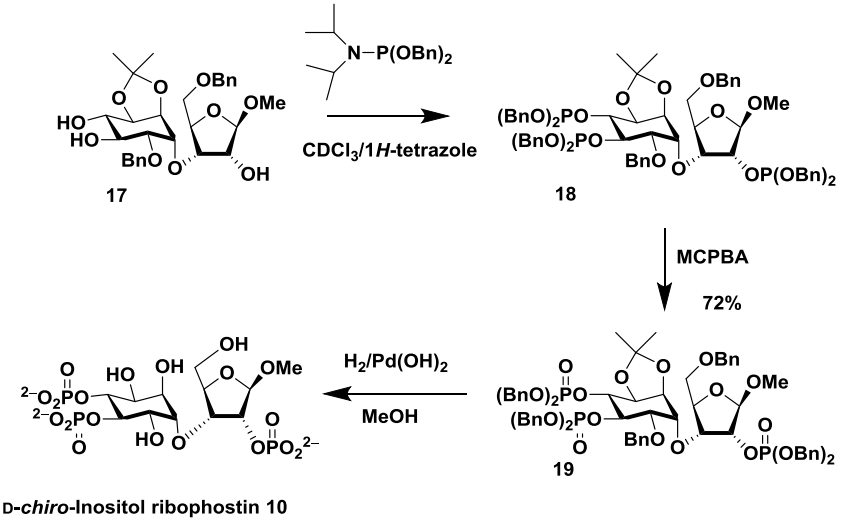

bisphosphate motif mimics the Ins(1,4,5)P_3 vicinal bisphosphate, while the 2″-hydroxyl and 2′-phosphate groups mimic the nonessential 6-hydroxyl[26] and the 1-phosphate of Ins(1,4,5)P_3, respectively. A recently published cryo-electron microscopy (EM) structure[2] of Ins(1,4,5)P_3R1 with bound adenophostin A hints at substantially different binding modes for this ligand. However, the ligand resolution in these protein structures is poor, the adenophostin A structure shown is incorrect (the pentose sugar is shown as xylose rather than a ribose derivative), and it is puzzling that the occupancy of the IBC by adenophostin A is very low in the presence of a saturating concentration of the ligand.[2] Until these data are validated, we continue to work with our hypothesis that the glucose 2″-hydroxyl and 3″,4″-bisphosphate triad motif of adenophostin A and related motifs in the corresponding disaccharide analogues discussed below mimic the respective 6-OH and 4,5-bisphosphate motifs of Ins(1,4,5)P_3 (Figure 1).

The simplest adenophostin A derivative designed to date is the glucopyranoside 2′,3,4-trisphosphate [Glc(2′,3,4)P_3] (**5**, Figure 2), in which the adenine and part of the ribose (C-1, C-4, and C-5 of ribose) were removed, leaving only an hydroxyethylphosphate moiety tethered at the α-anomeric position of glucose.[27,28] Glc(2′,3,4)P_3 was ca. 10-fold less potent than Ins(1,4,5)P_3 in releasing Ca^{2+} through Ins(1,4,5)P_3R,[19] confirming the likely importance of the adenine and entire ribose sugar of adenophostin A. Others confirmed similar activity for Glc(2′,3,4)P_3 and showed that it is not degraded by either of the enzymes that metabolize Ins(1,4,5)P_3, the 5-phosphatase and 3-kinase.[29] The ribose sugar tethered at the anomeric center of glucose was reintroduced to give ribophostin (**6**), which has also a β-OMe group replacing the adenine base at position-1 of ribose, and furanophostin (**7**), in which the anomeric OMe group and the methylene hydroxyl (at C-5 on ribose) were removed (Figure 2). The potency of both **6** and **7** was similar to that of Ins(1,4,5)P_3.[11] Further pruning of furanophostin by removal of the pyranoside methylene hydroxyl group to give **8** reduced the potency to ca. 3-fold below that of Ins(1,4,5)P_3.[11,30] Hence, ribophostin and furanophostin probably provide the best minimal disaccharide-based mimics of Ins(1,4,5)P_3. Compound **9** with the same phosphorylated tetrahydrofuran motif as **8**, but with β-stereochemistry at the hemiacetal, was inactive,[30] confirming an essential α-stereochemical requirement for ribophostin.

Since D-*chiro*-inositol adenophostin **4** is more potent than adenophostin A,[20] we speculated that replacing the glucose motif of ribophostin with a D-*chiro*-inositol derivative might also increase the potency of **6**. We now report a synthesis of D-*chiro*-inositol ribophostin **10** and demonstrate that it both binds with greater affinity than ribophostin to Ins(1,4,5)P_3R and more potently evokes Ca^{2+} release, confirming the value of our approach. Moreover, the potency difference between **6** and **10** is considerably greater than that observed between **2** and **4**, and unlike Ins(1,4,5)P_3, **10** is efficacious and exhibits metabolic resistance in an assay using patch-clamped whole cells.

RESULTS AND DISCUSSION

Chemistry. Previously, we discussed why a rigidly protected *myo*-inositol ring was key for the synthesis of D-*chiro*-inositol adenophostin[20] and that a rigid inositol triflate L-3-*O*-trifluoromethylsulfonyl-6-*O*-*p*-methoxybenzyl-1,2:4,5-di-*O*-isopropylidene-*myo*-inositol **11** can undergo an S_N2 reaction with a hard nucleophilic ribose derivative as its anion. Thus, triflate **11** (vide infra for an alternative formal identification of its absolute configuration as employed here) was coupled with the known suitably protected ribose derivative **12**[20,31] in tetrahydrofuran (THF)-hexamethylphosphoramide (HMPA) with NaH as base[20] (Scheme 1). The fully protected ribose–inositol *sec*–*sec* ether derivative **13** was formed in a reasonable yield (62%), and the more acid-sensitive *trans*-isopropylidene was then removed selectively and rapidly in the presence of ethylene glycol and catalytic *p*-toluenesulfonic acid (10–15 min) to give diol **14** in 85% yield. The presence of the ribose now attached to the D-*chiro*-inositol derivative via an ether seemed to affect the ease with which the *trans*-isopropylidene acetal was removed by acid in the presence of ethylene glycol. Possibly, the axial ribose of derivative **13** may increase the strain of the *trans*-acetal and could facilitate its removal. Our previous studies[32] showed that a longer reaction time (40 min) and more tetraol (from removal of both diol-protecting groups) resulted from a simple 1,2:4,5-di-*O*-isopropylidene

https://dx.doi.org/10.1021/acs.jmedchem.9b01986
J. Med. Chem. 2020, 63, 3238–3251

Scheme 3. Determination of the Absolute Configuration of the Partially Protected D-1,2:4,5-di-*O*-isopropylidene-*myo*-inositol Diol 22 from the Separated Diastereoisomer 20

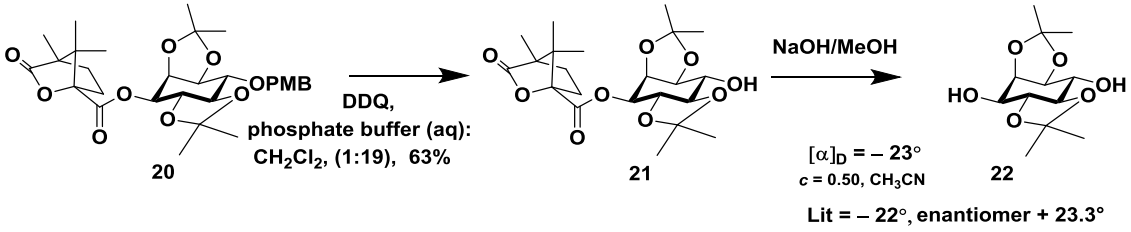

derivative with allyl protection at the 3- and 6-positions. Monobenzylation was then achieved by the formation of a tin acetal on diol **14** in the presence of dibutyltin oxide. The addition of cesium fluoride and excess benzyl bromide gave the separable monobenzylated products **15** and **16** in roughly equal amounts, demonstrating that no selective monobenzylation was achieved under these conditions. Compound **16** was identified by ^{1}H NMR spectroscopy since it showed a double triplet where the proton at C-3-H (of the D-*chiro*-inositol motif) flanked by two adjacent axial protons also had an extra coupling to the hydroxyl group C-3-OH that exchanged with D_2O. If the exchangeable OH was at C-2-H, next to the axial ribose−inositol ether bond, there should be a double double doublet, which upon exchange should give a double doublet. The next step required the removal of the two *p*-methoxybenzyl groups. Deprotection under acidic conditions was not an option as this would also remove the *cis*-isopropylidene moiety. Thus, 2,3-dichloro-5,6-dicyano-1,4-benzoquinone (DDQ) in dichloromethane−water was used, giving the protected triol **17** for phosphorylation in a reasonable yield (63%) after 1 h (Scheme 1).

Phosphitylation of **17** in $CDCl_3$ provided trisphosphite **18** (Scheme 2). ^{31}P NMR spectroscopy showed the expected AB system for the vicinal bisphosphite motif,[33] with one half centered around δ = 140.5 and the other at δ = 138.8, J = 6.0 Hz. Intermediate **18** was then oxidized with *m*CPBA to give the trisphosphate **19** in good yield (72%). Compound **19** was then deblocked at room temperature using palladium hydroxide and hydrogen. The best deprotection method was to leave the mixture stirring for 1 week at room temperature; the isopropylidene group was removed due to the acidic nature of the adjacent phosphates. Purification of the product, first using a gradient of triethylammonium bicarbonate (TEAB) buffer, then over RP18 resin, provided the target trisphosphate **10** in 43% yield. The product was quantified for biological assays after RP18 purification using the Briggs test.[34,35]

The synthesis and separation of camphanate **20**, leading to compound **22** and the more polar camphanate derivative (not shown but used to synthesize compound **11**), were discussed previously.[20] The *p*-methoxybenzyl (PMB) group of **20** was first removed using DDQ in a dichloromethane−phosphate buffer. Since **22** is highly soluble in both dichloromethane and water, it would be difficult to extract and purify. The reaction was also buffered because the *trans*-4,5-isopropylidene group may be easily removed from **20** in its conversion to **21** in the presence of the acidic phenol $DDQH_2$. The camphanate derivative was then deacylated in methanolic sodium hydroxide. The less polar diastereoisomer was identified as being a derivative of D-1,2:4,5-di-*O*-isopropylidene-*myo*-inositol **22**, by virtue of its rotation, and close to the literature values.[36−38] The other, more polar diastereoisomeric camphanate was isolated by chromatography, then deacylated, as previously described,[20] giving L-6-*O*-*p*-methoxybenzyl-1,2:4,5-di-*O*-isopropylidene-*myo*-inositol, and used for the synthesis of inositol triflate **11** (Scheme 3).

Biology. In permeabilized avian DT40 cells expressing only rat Ins(1,4,5)P_3R1 (DT40-Ins(1,4,5)P_3R1 cells), maximally effective concentrations of Ins(1,4,5)P_3 **1**, ribophostin **6**, and D-*chiro*-inositol ribophostin **10** each released the same fraction (ca. 65%) of the intracellular Ca^{2+} stores. Ins(1,4,5)P_3 and ribophostin were equipotent, but D-*chiro*-inositol ribophostin was ca. 7-fold more potent than ribophostin (Figure 3 and

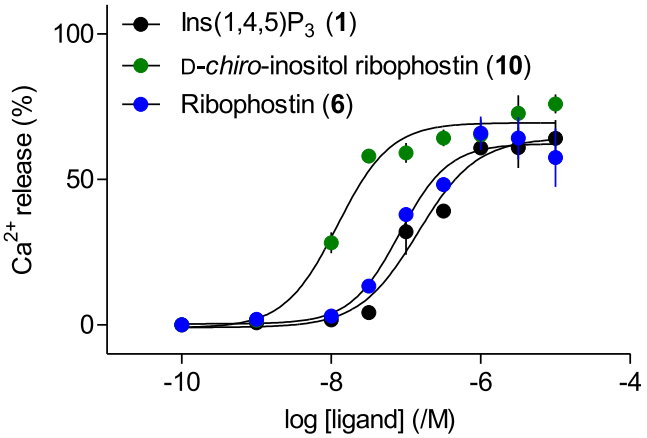

Figure 3. Effects of ligands on Ca^{2+} release from the intracellular stores of permeabilized DT40-Ins(1,4,5)P_3R1 cells. Results, expressed as a percentage of the Ca^{2+} content of the intracellular stores, show the effects of the indicated concentrations of each ligand. Mean ± SEM from three independent experiments (summarized in Table 1).

Table 1). Similar results were obtained from analyses of Ca^{2+} release in permeabilized mammalian cells expressing only rat Ins(1,4,5)P_3R1 (HEK-Ins(1,4,5)P_3R1 cells), where **1**, **2**, **6** and **10** each released the same fraction (ca. 70%) of the intracellular stores, and D-*chiro*-inositol ribophostin was 3-fold more potent than ribophostin and only 2-fold less potent than adenophostin A (Figure 4 and Table 2).

In equilibrium-competition binding assays using [^{3}H]-Ins(1,4,5)P_3 and cerebellar membranes, which express large amounts of Ins(1,4,5)P_3R1s, the affinity of D-*chiro*-inositol ribophostin for Ins(1,4,5)P_3Rs (defined by the equilibrium dissociation constant, K_d) was 2.3-fold greater than that of ribophostin and only 2-fold lower than that of adenophostin A (Figure 5 and Table 2). As reported previously,[39] a comparison of the ratio of the concentrations of ligand required to evoke half-maximal Ca^{2+} release (EC_{50}) and occupy 50% of Ins(1,4,5)P_3Rs (K_d), the EC_{50}/K_d ratio, can be used to report efficacy, that is, the ability of a ligand to activate Ins(1,4,5)P_3R

https://dx.doi.org/10.1021/acs.jmedchem.9b01986
J. Med. Chem. 2020, 63, 3238−3251

Table 1. Effects of Ligands on Ca^{2+} Release through Ins(1,4,5)P_3R1 Expressed in DT40 Cells[a]

	pEC_{50} (EC_{50}) (nM)	Ca^{2+} release (%)	*h*
Ins(1,4,5)P_3 (**1**)	6.88 ± 0.18 (133)	63 ± 5	2.0 ± 0.8
D-*chiro*-inositol ribophostin (**10**)	7.93 ± 0.06 (12)	70 ± 2	1.6 ± 0.4
ribophostin (**6**)	7.05 ± 0.10 (88)	64 ± 7	1.4 ± 0.4

[a]Results (from Figure 3) show mean ± standard error of the mean (SEM) (pEC_{50}, Ca^{2+} release (%) and *h*) and means (EC_{50}) from three independent experiments. EC_{50}, half-maximal effective concentration; pEC_{50}, -logEC_{50}; *h*, Hill coefficient. *$P < 0.05$ was considered significant. None of the mean values for Ca^{2+} release or *h* differed significantly between ligands. There were significant differences between pEC_{50} values for Ins(1,4,5)P_3 versus D-*chiro*-inositol ribophostin and ribophostin versus D-*chiro*-inositol ribophostin **10**.

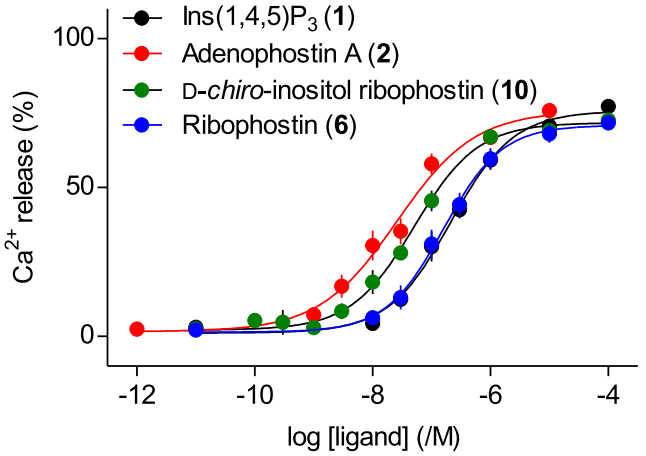

Figure 4. Effects of ligands on Ca^{2+} release from the intracellular stores of permeabilized HEK-Ins(1,4,5)P_3R1 cells. Results show mean ± SEM from nine independent experiments, each performed in duplicate (summarized in Table 2).

once it has bound. The ratios were similar for all four ligands (Table 2), and since Ins(1,4,5)P_3 and adenophostin A are full agonists,[39] we conclude that ribophostin and D-*chiro*-inositol ribophostin are also full agonists.

These results demonstrate that replacing the glucose moiety of ribophostin with an inositol substantially increases the affinity of the resulting ligand, D-*chiro*-inositol ribophostin, for Ins(1,4,5)P_3Rs without compromising efficacy. D-*chiro*-Inositol

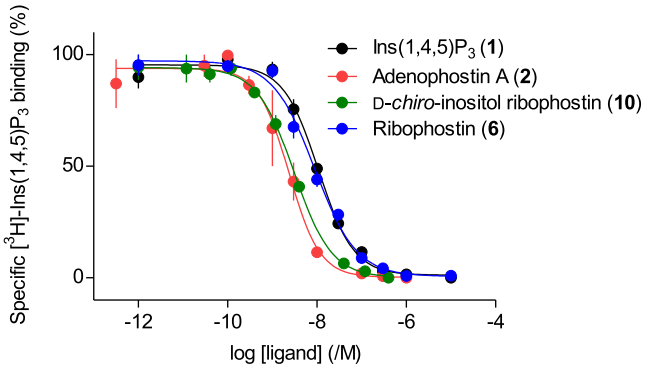

Figure 5. Equilibrium-competition binding to cerebellar membranes using [^{3}H]-Ins(1,4,5)P_3 and the indicated concentrations of competing ligands. Results show mean ± SEM from three independent experiments (summarized in Table 2).

ribophostin is the most potent ribophostin-type analogue synthesized to date.

Structure–Activity Relationships (SAR). Structure–activity relationship (SAR) parameters are summarized in Figure 6, and those for Ins(1,4,5)P_3 have been well rehearsed[5,7] (Figure 6a). Adenophostin A data (Figure 6b) are also more relevant for considering the activity of **10** since it possesses the core disaccharide motif of ribophostin (Figure 6c). Figure 6 demonstrates that apparently similar structural modifications do not necessarily correlate across the three ligand classes. Since compound **10** is a hybrid of Ins(1,4,5)P_3 and ribophostin and approaching the potency of adenophostin for Ca^{2+} release, a summary of the various strategic functional groups and the effect of various positional modifications within these molecules is given in Figure 6.

Exploration of a potential "supra-optimal" phosphate group in adenophostin A led to the synthesis of phosphorylated disaccharides[40] with conformational restriction, for example, sucrose 3,4,3′-trisphosphate (**23**), α,α′-trehalose 2,4,3′,4′-tetrakisphosphate (**24**), and α,α′-trehalose 3,4,3′,4′-tetrakisphosphate (**25**) (Figure 7). Comparing the three structures for optimal positioning of the single phosphate to that of the 2-phosphate on the ribose of ribophostin, compound **23** is 25-fold less potent for Ca^{2+} release, and therefore with the phosphate not in an optimal position. Compound **24** is only 6-fold weaker for Ca^{2+} release than ribophostin,[40] and compound **25** is 11.5-fold weaker for Ca^{2+} release and less potent than **24**.

The Ins(1,4,5)P_3R binding[21] model suggested mimicry of the key structural components of Ins(1,4,5)P_3, with binding

Table 2. Comparison of Binding and Functional Effects of Ins(1,4,5)P_3R Ligands[a]

	Ca^{2+} release			binding		
	pEC_{50} (EC_{50}) (nM)	release (%)	*h*	pK_d (K_d) (nM)	*h*	EC_{50}/K_d (95% CI)
Ins(1,4,5)P_3 (**1**)	6.68 ± 0.09 (209)	76 ± 2	1.0 ± 0.1	8.06 ± 0.03 (8.71)	1.1 ± 0.2	**24** (11–56)
adenophostin A (**2**)	7.57 ± 0.11 (27)	76 ± 3	1.0 ± 0.3	8.86 ± 0.14 (1.38)	1.2 ± 0.2	**19** (6–58)
D-*chiro*-inositol ribophostin (**10**)	7.28 ± 0.12 (52)	71 ± 1	1.1 ± 0.1	8.49 ± 0.03 (3.24)	1.0 ± 0.1	**16** (5–49)
ribophostin (**6**)	6.81 ± 0.10 (155)	72 ± 2	1.0 ± 0.1	8.12 ± 0.03 (7.59)	0.9 ± 0.1	**20** (8–51)

[a]Summary of the effects of ligands on Ca^{2+} release from the intracellular stores of HEK-Ins(1,4,5)P_3R1 cells (from Figure 4) and on [^{3}H]-Ins(1,4,5)P_3 binding to cerebellar membranes (from Figure 5). Results show mean ± SEM (pEC_{50}, Ca^{2+} release (%), pK_d and *h*) and means (EC_{50}, K_d) from nine (Ca^{2+} release) or three (binding) experiments. EC_{50}/K_d ratios show means with 95% confidence intervals (CI). $P < 0.05$ was considered significant. None of the mean values for Ca^{2+} release, *h* or EC_{50}/K_d ratios, differed significantly between ligands. There were significant differences between mean pEC_{50} values for Ins(1,4,5)P_3 versus adenophostin A, Ins(1,4,5)P_3 versus D-*chiro*-inositol ribophostin, adenophostin A versus ribophostin and D-*chiro*-inositol ribophostin versus ribophostin; and between mean pK_d values for Ins(1,4,5)P_3 versus adenophostin A, Ins(1,4,5)P_3 versus D-*chiro*-inositol ribophostin, and adenophostin A versus ribophostin.

https://dx.doi.org/10.1021/acs.jmedchem.9b01986
J. Med. Chem. 2020, 63, 3238–3251

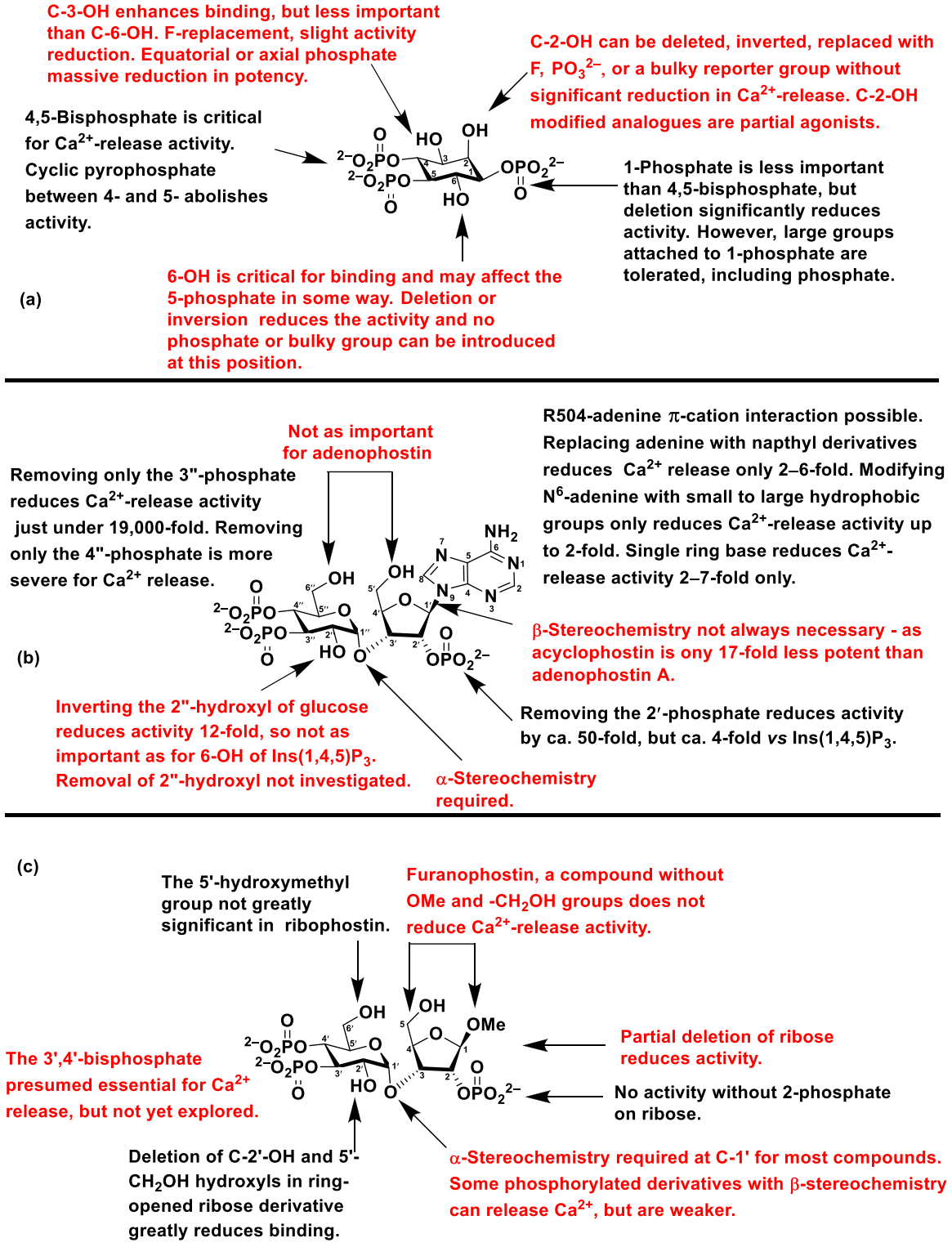

Figure 6. Comparative summary of structure–activity parameters for analogues of (a) Ins(1,4,5)P_3, (b) adenophostin A, and (c) ribophostin illustrating major differences between the three ligand classes.

enhanced by the adenine base of adenophostin A interacting with Arg504. This is supported by mutagenesis data.[12] The N6 position can be modified with little effect on activity[21] and, while substantial modifications to the adenine base are tolerated,[16,17,41] a bicyclic ring system is preferred. The two sugar hydroxymethyl groups are not important for potent activity, and ribose 2′-phosphate, while not critical, mimics the 1-phosphate of Ins(1,4,5)P_3.[11] The idea that this phosphate may facilitate binding in a supra-optimal fashion was discounted in favor of synergy between the adenine base and the phosphate group.[12] The vicinal glucose bisphosphate is critical for potent activity, and removing either the 3′-phosphate or 4″-phosphate massively decreases activity, but the 4′′-phosphate is less critical.[11,13,22] Acyclophostin **26**, an analogue that can be viewed as either an "opened" ribose or similar to **5** but with an additional adenine motif, is only 14–

https://dx.doi.org/10.1021/acs.jmedchem.9b01986
J. Med. Chem. 2020, 63, 3238–3251

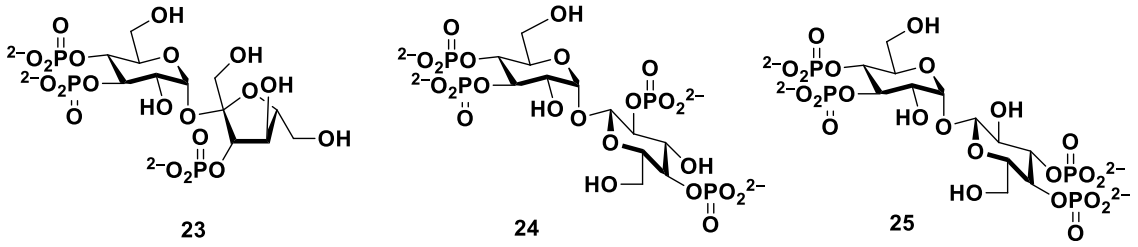

Figure 7. Disaccharide polyphosphate agonists to explore conformational restriction.

17-fold less potent than adenophostin A[42] and a pH-dependent partial agonist. Transposing the 3″-phosphate of adenophostin to the glucose 2′′-hydroxyl group gave a 2,2′,4-trisphosphate **27** (Figure 8) that is surprisingly only 12-fold less potent than

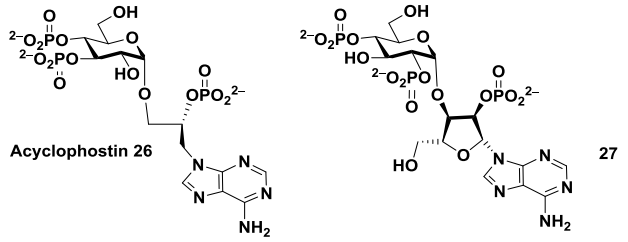

Figure 8. Structures of the ribose ring-opened adenophostin analogue acyclophostin **26** and the active regioisomeric 2,2′,4-trisphosphate adenophostin analogue **27**.

$Ins(1,4,5)P_3$ and was perhaps the most surprising of all analogues to date.[42] However, with an understanding of the structure of the IBC, this could subsequently be rationalized without disturbing the original binding model.[13,21]

Figure 6c illustrates the SAR for ribophostin for which modifications have been synthesized. The skeletal tetrahydrofuran derivative such as **8** (Figure 2) exhibits a potency close to $Ins(1,4,5)P_3$ and ribophostin.[11] There is little effect when the primary hydroxymethyl groups are removed either individually or together.[19] If 3,4-bisphosphate is replaced with bis-phosphorothioate,[19] EC_{50} drops 5-fold.

Compound **28** (Figure 9) is a diastereoisomer of compound **8** (Figure 2). **28** has a very low potency in Ca^{2+}-release assays,[19,30] and **29**, with β-stereochemistry, releases Ca^{2+} with only ~19-fold lesser potency than $Ins(1,4,5)P_3$.[19,30] The reasons for this are unclear. Xylopyranoside 2′,3,4-trisphosphate **30** has 17-fold lower affinity than $Ins(1,4,5)P_3$, but 2-deoxy-xylopyranoside 2′,3,4-trisphosphate **31** has 2000-fold lower affinity, indicating the importance of the pyranose 2-hydroxyl group (equivalent to the C-6-OH of $Ins(1,4,5)P_3$).[43]

Thus, all three ligands exhibit diverse SAR features and, while these structural modifications on activity individually have been extensively reviewed,[5,44] they have not before been juxtaposed between analogue classes as in Figure 6.

Two sterically constrained phosphorylated epimers (*R*)-**32** and (*S*)-**33** and the "spirophostin" compounds (*R*)-**34** and (*S*)-**35** were also synthesized (Figure 10).[45,46] **32** and **33** were,

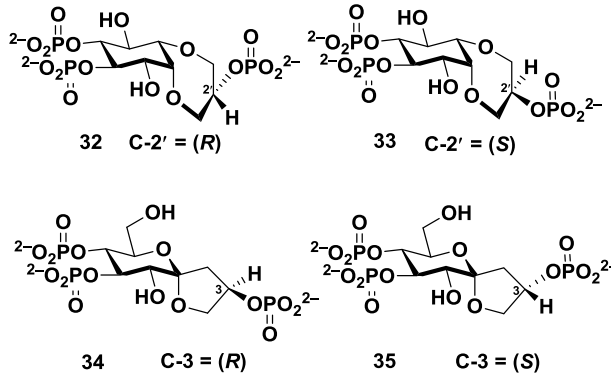

Figure 10. Synthetic sterically constrained epimers to explore the conformational restriction at the potentially supraoptimal nonvicinal phosphate group.

respectively, 18- and 14-fold less potent than $Ins(1,4,5)P_3$, and **34** and **35** were 6-fold and ca. 12-fold less potent for Ca^{2+}-release. No compound (**28**–**35**) is as potent as ribophostin, which behaves similarly to $Ins(1,4,5)P_3$.[40]

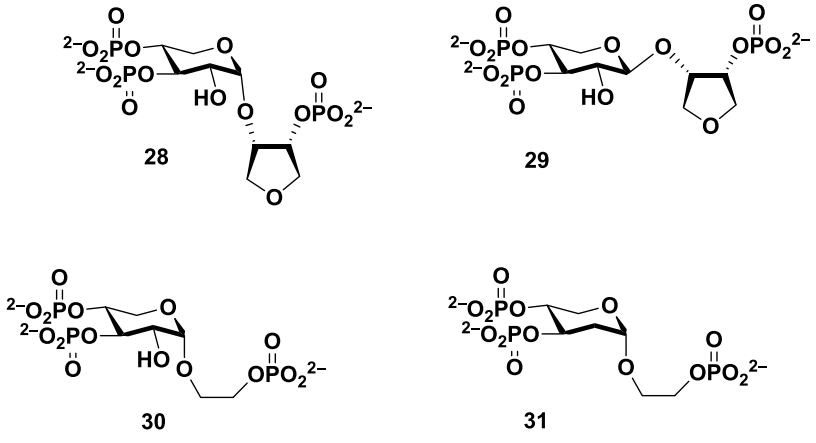

Figure 9. Structures of minimal xylopyranoside-based agonists.

https://dx.doi.org/10.1021/acs.jmedchem.9b01986
J. Med. Chem. 2020, 63, 3238−3251

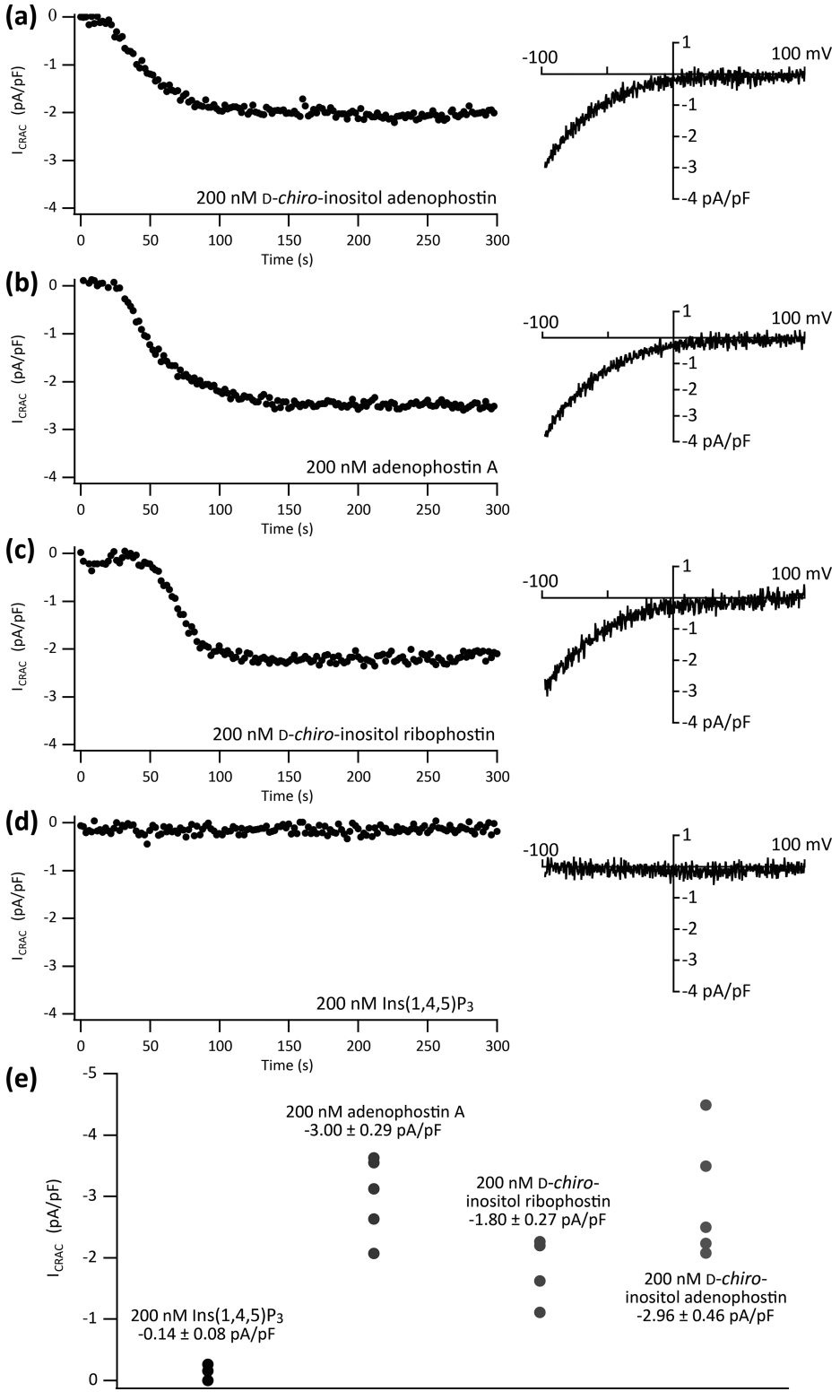

Figure 11. Activation of the store-operated Ca^{2+} current I_{CRAC} in RBL-2H3 cells following whole-cell dialysis with the Ins(1,4,5)P_3R ligands (a) D-*chiro*-inositol adenophostin **4**, (b) adenophostin A **2**, (c) D-*chiro*-inositol ribophostin **10**, and (d) Ins(1,4,5)P_3**1**. Representative time courses (measured at ÷ 80 mV) and current−voltage relationships are shown. 200 nM Ins(1,4,5)P_3 routinely failed to evoke a detectable whole-cell current. Data are summarized in (e) as mean ± SEM, three to five cells for each condition.

D-*chiro*-Inositol adenophostin **4** was the first adenophostin A analogue of its kind to possess a glucose-to-inositol replacement, offering increased possibilities for structural diversity and engineering by virtue of its extra hydroxyl group replacing the pyranoside oxygen. It was more active than adenophostin A itself, albeit by a relatively modest margin.[20] The simplest interpretation is that the D-*chiro*-inositol trisphosphate moiety of **4** better fits into the receptor than the glucose-based mimic of adenophostin A, consistent with our original binding model.[21] Similarly, D-*chiro*-inositol

https://dx.doi.org/10.1021/acs.jmedchem.9b01986
J. Med. Chem. 2020, 63, 3238−3251

ribophostin **10** is the first ribophostin analogue of its kind where the glucose 3,4-bisphosphate moiety is replaced with a D-*chiro*-inositol 3,4-bisphosphate unit. Different chemistry is used to form the hemiacetal of ribophostin **6** and the *sec*−*sec* ether of **10**. The main difference between **6** and **10** is that the 5- and 6-positions of D-*chiro*-inositol (mimicking the 3- and 2-positions of Ins(1,4,5)P_3 in our model[20]) replace the 5-hydroxymethyl group and the pyranoside oxygen. Figure 6a−c shows how individual positions on Ins(1,4,5)P_3, ribophostin, and adenophostin influence activity. It might be expected from this that there would be little gain in activity by replacing a pyranoside oxygen by a C2−OH group. Similarly, the loss of a hydroxymethyl group would not be expected to greatly affect activity, and its replacement by an inositol hydroxyl group should not have any marked effect.

In practice, however, the effects are more marked than expected and exceed those observed in the case of **4**. When the potency of adenophostin A **2** is compared to that of its counterpart inositol adenophostin **4**, **4** is some 1.6-fold more potent in Ca^{2+}-release assays.[20] Similarly, replacing the glucose unit of ribophostin with an inositol motif enhances potency, but more appreciably. Thus, in Ca^{2+}-release assays in two systems, inositol ribophostin **10** was ca. 7- and 3-fold more potent than ribophostin **6** and 11-fold and 4-fold more potent than Ins(1,4,5)P_3, approaching adenophostin A in its activity. **10** also had a greater affinity than Ins(1,4,5)P_3 for Ins(1,4,5)-P_3R1. Thus, glucopyranoside replacement can further increase the biological activity, presumably through a better fit of the new inositol bisphosphate moiety with the receptor than the original glucose bisphosphate mimic derived from adenophostin A. Perhaps also the lack of a base motif as in **4** allows more conformational flexibility for **6** in its search for an optimal binding conformation. It is conceivable, therefore, from our binding model[21] and related work implicating a specific role for the adenine base of adenophostin[12,13,18,22,23] that conformational movement of adenophostin **2** (and therefore perhaps also of inositol adenophostin **4**, if assumed to bind similarly in the nucleotide region) may be more restricted in its extended binding mode, influencing options available for the glucose or inositol bisphosphate components. By contrast, the simpler **4** could be more flexible and more able to optimize its fit in the likely more important region of Ins(1,4,5)P_3R. Note also that when comparing ribophostin **6** with Ins(1,4,5)P_3 **1** in activity, the former appears to be ca. 1.3- to 1.5-fold more potent. The precise reasons why a ligand without an adenine base, but now based on an inositol−sugar polyphosphate hybrid rather than a sugar−sugar counterpart, should significantly exceed Ins-(1,4,5)P_3 in potency need further investigation. Since the conformation of disaccharides and a polyphosphate derivative such as **6** is mainly determined by the populations of rotamers around the glycosidic linkage, it could be pertinent to consider how changing this linkage to a *sec*−*sec* ether in **10** might change this. However, **10** appears to be the most potent simple (i.e., nondimeric and non-adenophostin A-based) small-molecule Ca^{2+}-mobilizing analogue yet synthesized. Also, its possession of an axial Ins(1,4,5)P_3 2-hydroxyl mimic, in place of a pyranoside oxygen as in **4** affords the same extra synthetic flexibility for further structural elaboration that might allow access to the cleft of the Ins(1,4,5)P_3R clam by a suitably tailored pendant group.

We also compared the relative abilities of **10** and its nucleotide parent **4** in a functional sense to activate I_{CRAC} in rat basophilic leukemia RBL-2H3 cells in comparison to Ins-(1,4,5)P_3 and adenophostin A. We selected a concentration of 200 nM for Ins(1,4,5)P_3 because this dose is just below the threshold for I_{CRAC} activation.[47] Dialysis with 200 nM adenophostin A evoked a large I_{CRAC} after a short delay (Figure 11b), as reported previously.[47,48] The current−voltage relationship, taken at steady state, is shown on the right and reveals the strong inward rectification and positive reversal potential that are hallmarks of I_{CRAC}. Current amplitude from several cells is shown in the plot in Figure 11e. Inositol adenophostin **4** activated I_{CRAC} with similar kinetics to adenophostin A, and the amplitude of the current (at −80 mV) was similar to that evoked by adenophostin A (Figure 11a). Inositol ribophostin **4** also activated I_{CRAC} but after a slightly longer delay, and the current typically attained a smaller amplitude (Figure 11d). We thus demonstrate for the first time that inositol adenophostin **4** is able to elicit a functional store-operated Ca^{2+} current I_{CRAC} in patch-clamped cells, similar to adenophostin A **2** (Figure 11b), an activity downstream of the Ins(1,4,5)P_3R, whereas Ins(1,4,5)P_3 itself (Figure 11d) is inactive. Inositol ribophostin **10** (Figure 11c) is also able to stimulate this current. As is apparent from Figure 11e, inositol adenophostin is thus functionally similar to adenophostin and both are slightly more potent than inositol ribophostin. All three are considerably more potent than Ins(1,4,5)P_3 under these conditions with its lack of activity presumably the result of extensive metabolism. This confirms not only the high activity of **10** but suggests it to be substantially hydrolysis-resistant in whole cells, potentially enhancing its value along with **4** as an investigative tool for chemical biology.

CONCLUSIONS

In summary, a concise first synthesis of D-*chiro*-inositol ribophostin **10**, an inositol-based counterpart of the glyconucleotide natural product adenophostin analogue ribophostin has been achieved. Key features include coupling of a chiral-protected *myo*-inositol diol derivative activated as its triflate **11** to the chiral-protected ribose derivative **12**. The chiral diol D-(−)-1,2:4,5-di-*O*-isopropylidene-*myo*-inositol **22**,[36−38] derived from the separable diastereoisomeric 3-*O*-camphanate derivative of its 6-*O*-*p*-methyoxybenzyl ether, was used to define the absolute configuration of **11** by comparison with the literature values. Subsequent elaboration of the coupled product after deprotection of the labile isopropylidene group and monobenzylation of the stannylene-mediated vicinal hydroxyl group with separation and identification of regioisomers afforded a suitably protected triol **17**. After phosphitylation and oxidation, the removal of all protecting groups afforded the target **10** that was evaluated as an agonist for intracellular Ca^{2+} release through the Ins(1,4,5)P_3R in permeabilized cells stably expressing Ins(1,4,5)P_3R1. D-*chiro*-Inositol ribophostin was more potent than Ins(1,4,5)P_3 and, more particularly, its disaccharide parent ribophostin surprisingly approached adenophostin A in activity, being only ca. 2-fold weaker. This was also confirmed using equilibrium-competition binding studies using displacement of [^{3}H]-Ins(1,4,5)P_3. Thus, glucopyranoside-inositol replacement can further optimize biological activity, presumably by facilitating a better fit to Ins(1,4,5)P_3R than a pyranoside-based mimic directly based on the natural product adenophostin A. **10** is the most potent simple analogue agonist of Ins(1,4,5)P_3R so far identified that does not possess the adenine base motif of adenophostin A thought to enhance receptor binding. Moreover, using the

https://dx.doi.org/10.1021/acs.jmedchem.9b01986
J. Med. Chem. 2020, 63, 3238−3251

patch-clamp methodology, **10** was shown to elicit a downstream store-operated Ca^{2+} current like adenophostin A, demonstrating both its efficacy and metabolic stability. Ins(1,4,5)P_3 under the same conditions showed no response and is presumably heavily metabolized. This further underlines the potential of such ligands as chemical biology tools. Structure−activity implications are discussed in the context of Ins(1,4,5)P_3, adenophostin A, and ribophostin. D-*chiro*-Inositol ribophostin thus represents a new class of simple but highly potent Ins(1,4,5)P_3 analogue as a phosphorylated inositol−sugar conjugate that may be useful for further development and chemical biology applications.

EXPERIMENTAL SECTION

Ca^{2+}-Release Assays. The methods used to measure Ca^{2+} release from the intracellular stores of permeabilized HEK or DT40 cells stably expressing only Ins(1,4,5)P_3R1 were exactly as reported previously.[11,20] Briefly, stable cell lines expressing rat Ins(1,4,5)P_3R1 were established from cells in which all endogenous Ins(1,4,5)P_3R genes had been disrupted. The intracellular stores were loaded with a low-affinity fluorescent Ca^{2+} indicator (Mag-fluo4), the plasma membrane of the cells was then permeabilized by incubation with saponin, and the intracellular stores were loaded with Ca^{2+} by incubating cells in 96-well plates in a cytosol-like medium containing ATP. A FlexStation III plate-reader was used to record Mag-fluo4 fluorescence at 1.44 s intervals during Ca^{2+} loading and then in the presence of cyclopiazonic acid, to inhibit further Ca^{2+} uptake, added either with the Ins(1,4,5)P_3R ligands (DT40 cells) or 60 s before addition of the ligands (HEK cells). Ca^{2+} release was calculated as a percentage of the fluorescence signal from fully loaded stores (F_{full}) minus the signal from empty stores ($F_{full} - F_{empty}$).

[^{3}H]-Ins(1,4,5)P_3 Binding Assays. Equilibrium competition binding to membranes prepared from rat cerebellum was performed in a medium comprising 50 mM Tris, 1 mM ethylenediaminetetraacetic acid (EDTA), pH 8.3 with [^{3}H]-Ins(1,4,5)P_3 (19.3 Ci/mmol, 1.5 nM), and the competing ligand and evaluated exactly as reported previously.[39]

Data Analysis. Concentration−effect relationships and equilibrium competition-binding results were fitted to Hill equations (GraphPad Prism, version 5), and EC_{50}/K_d ratios were processed as previously described.[39] Statistical analysis used analysis of variance (ANOVA) followed by Bonferroni's multiple comparison test (GraphPad Prism, version 5). $P < 0.05$ was considered significant.

Electrophysiology. Patch clamp experiments were conducted on rat basophilic leukemia RBL-2H3 cells (ATCC CRL-2256) in the tight seal whole-cell configuration at room temperature (20−24 °C) as previously described.[47] Pipettes were pulled from borosilicate glass and then Sylgard-coated and fire-polished. They had resistances of 4−6 MΩ when filled with an internal solution containing (mM) 145 Cs glutamate, 8 NaCl, 1 $MgCl_2$, 10 HEPES, 0.35 EGTA, 2 Mg-ATP, pH 7.2 (CsOH). The internal solution was supplemented with 200 nM Ins(1,4,5)P_3, adenophostin A, inositol adenophostin, or inositol ribophostin, as indicated. The external solution contained (mM) 155 NaCl, 10 $CaCl_2$, 10 CsCl, 2.8 KCl, 2 $MgCl_2$, 10 HEPES, 10 glucose, pH 7.4 (NaOH). Whole-cell currents were filtered using an eight-pole Bessel filter at 2.5 kHz and digitized at 100 μs. The store-operated Ca^{2+} current I_{CRAC} was measured at −80 mV from voltage ramps spanning −100 to +100 mV (50 ms duration, 0.5 Hz, 0 mV holding potential). Whole-cell currents were normalized to cell capacitance. Capacitative currents were automatically compensated for before each ramp by the EPC 9−2 amplifier (HEKA, Lambrecht/Pfalz, Germany). Leak currents were removed by subtracting the first one to five ramps obtained immediately after break-in.

Chemistry. Chemicals were purchased from Acros Organics, Alfa Aesar, Fisher Scientific, and Sigma-Aldrich. thin-layer chromatography (TLC) was carried out on Merck TLC aluminum sheets coated with silica 60F_{254}. The products were developed by dipping a TLC plate in an ethanolic solution of phosphomolybdic acid, and then heated at a high temperature. Flash chromatography was performed using silica 60 A (Fisher Scientific). Hexamethylphosphoramide (HMPA) was dried over calcium hydride and distilled under pressure. Organic solutions of compounds were dried over dry $MgSO_4$. All compounds were characterized by spectroscopic methods (NMR and MS), and the final compound was purified using ion-exchange chromatography with a LKB-Pharmacia Medium Pressure Ion Exchange Chromatograph using Q-Sepharose Fast Flow and a 0−2.0 M gradient of triethylammonium bicarbonate (TEAB) followed by purification over RP18 resin. Fractions containing the final compound were identified by the Briggs test,[34] and compounds were then quantified by this assay, using a standard curve. Briefly, column fractions containing a polyphosphate were assayed for phosphate by a modification of the assay as follows:[35] a molybdate solution (12.5 g of ammonium molybdate dissolved in 250 mL of water and 35 mL of concentrated H_2SO_4), a hydroquinone solution (0.5 g of hydroquinone dissolved in 100 mL of water and a drop of concentrated H_2SO_4), and a sulfite solution (20% w/v sodium sulfite in water) were prepared. Aliquots (250 μL) of the fractions were transferred into test tubes, concentrated H_2SO_4 (three drops) was added, and the samples were heated at 150 °C for 1 h. After cooling, water (500 μL), molybdate solution (500 μL), hydroquinone solution (250 μL), and sulfite solution (250 μL) were added and the samples were boiled for 7 s and allowed to cool. Phosphate-containing fractions were identified by their blue color. For quantitative analysis, samples containing known amounts of potassium dihydrogen phosphate were co-assayed with samples of unknown phosphate contents. After being processed as above, fractions were transferred to 10 mL volumetric flasks, water was added to give 10 mL of solution, and the UV absorbance at 340 nm was recorded using 3 mL quartz cells. The concentration of the unknown samples was calculated from a standard curve derived from the absorbances of the reference samples. Final compounds were used in biological assays after such quantification as their triethylammonium salts. All compounds were of purity >95% by NMR. ^{1}H NMR spectra were recorded at 400 MHz and 500 MHz, ^{13}C NMR spectra were recorded at 100 MHz and 125 MHz, and ^{31}P spectra at 202.4 MHz on a Varian Mercury VX400 NMR machine and a 500 MHz Bruker Advance III. Mass spectra were recorded on a Bruker MicrOTOF electrospray electrospray ionization time-of-flight (ESI-TOF) spectrometer with sodium formate as the standard. Melting points were recorded on a Systems Optimelt automated melting point system. Optical rotations were measured in an Optical Activity Ltd AA-10 polarimeter.

(3a*S*,4*S*,4a*S*,7a*R*,8*R*,8a*S*)-4-(((3*R*,4*R*,5*R*)-2-((Benzyloxy)-methyl)-5-methoxy-4-((4-methoxybenzyl)oxy)-tetrahydrofuran-3-yl)oxy)-8-((4-methoxybenzyl)oxy)-2,2,6,6-tetramethylhexahydrobenzo[1,2-*d*:4,5-*d*′]bis([1,3]dioxole) (13). Dry HMPA (2 mL) was added to methyl 5-*O*-benzyl-2-*O*-*p*-methoxybenzyl-β-D-ribofuranoside (**12**, 200 mg, 0.53 mmol) and NaH (25 mg, 95%, 1.0 mmol), and the mixture was stirred under argon for 30 min and cooled with ice. L-(+)-1,2:4,5-di-*O*-isopropylidene-6-*O*-*p*-methoxybenzyl-3-*O*-trifluoromethanesulfonyl-*myo*-inositol (**11**, 555 mg, 1.07 mmol) was added as a solid, and the remainder in the weighing vessel was washed with dry THF (2 mL). The reaction mixture turned orange/yellow, and the reaction was allowed to warm to room temperature as the ice melted. The reaction was allowed to slowly warm to lab temperature after the addition of the triflate, and the mixture was stirred overnight, for 17 h in total.

The THF was evaporated and the solution of HMPA was poured into a saturated solution of ammonium chloride (25 mL), and the solution was left to separate. The liquid part was decanted off, and this contained mainly the HMPA with a trace amount of product and starting material. The remaining solid products were extracted with ether (4 × 25 mL) after a further addition of saturated ammonium chloride (25 mL). Purification by chromatography 40−60 °C petroleum ether/EtOAc (2:1) provides the product (**13**, 241 mg, 62%). $[\alpha]_D$ = +33.33°, 20 °C, (c = 1.74, $CHCl_3$).

^{1}H NMR (500 MHz, $CDCl_3$) 1.24, 1.31, 1.33, 1.42 (12 H, 4 s, 4 × CH_3), 3.29 (3 H, s, ribose-O*Me*), 3.57−3.63 (3 H, m, CH_2OBn, 1 H, H-4-Ins), 3.73 (1 H, dd, J = 2.6, 10.0 Hz, H-2-Ins), 3.76 (3 H, s,

https://dx.doi.org/10.1021/acs.jmedchem.9b01986
J. Med. Chem. 2020, 63, 3238−3251

CH_2PhOMe), 3.80 (3 H, s, CH_2PhOMe), 3.88 (1 H, d, J = 4.5 Hz, H-2-ribose), 4.02 (1 H, t, J = 10.0 Hz, H-3-Ins), 4.19−4.25 (2 H, m, H-4-ribose, H-4-Ins), 4.32−4.35 (2 H, m, H-1-Ins, H-6-Ins), 4.39 (1 H, dd, J = 4.5, 7.2 Hz, H-3-ribose), 4.57−4.75 (6 H, m, CH_2Ph, CH_2PhOMe), 4.81 (1 H, s, H-1-ribose), 6.84−6.88 (4 H, m, 2 × CH_2PhOMe), 7.25−7.36 (9 H, m, CH_2Ph, CH_2PhOMe).

^{13}C NMR (125 MHz, $CDCl_3$) 25.73, 26.79, 27.20, 27.70 (4 q, 2 × $C(CH_3)_2$), 54.89, 56.24, 56.25 (3 q, 2 × CH_2PhOMe, ribose-OMe), 70.88, 71.46, 72.19, 73.37 (4 t, CH_2Ph, CH_2PhOMe, CH_2OBn), 72.80, 75.20, 76.69, 77.90, 79.78, 80.12, 80.37, 80.51, 81.76, 106.20 (10 × -C-H ring carbons for inositol and ribose), 109.25, 111.19 (C_q, 2 × $C(Me)_2$), 113.53, 113.81 (C-H, 2 × CH_2PhOMe), 127.53, 128.32, 129.27, 129.50 (d, C-H, CH_2Ph, CH_2PhOMe), 130.22, 130.59, 138.07 (C_q, s, CH_2Ph, CH_2PhOMe), 159.01, 159.21 (C_q, s, CH_2PhOMe). M/z $C_{41}H_{53}O_{12}$ $[M + H]^+$ expected 737.3532; found 737.3532: $C_{41}H_{52}NaO_{12}$ $[M + Na]^+$ expected 759.3351; found 759.3340.

(3a*S*,4*R*,5*R*,6*R*,7*S*,7a*R*)-4-(((3*R*,4*R*,5*R*)-2-((Benzyloxy)methyl)-5-methoxy-4-((4-methoxybenzyl)oxy)tetrahydrofuran-3-yl)oxy)-7-((4-methoxybenzyl)oxy)-2,2-dimethylhexahydrobenzo[*d*][1,3]dioxole-5,6-diol (14). The fully blocked compound (**13**, 381 mg, 517 μmoles) was dissolved in methylene chloride (25 mL) followed by the addition of a catalytic amount of PTSA (5 mg, 0.025 mmol) and ethane 1,2-diol (38 mg, 0.612 mmol), 1.18 equiv. The mixture was stirred at room temperature, and the reaction was complete within 10−15 min and monitored by TLC [EtOAc/petroleum ether (2:1)], R_f = 0.44 for the diastereoisomer **14**. The product was purified by flash chromatography using a combiflash and gradient of EtOAc/petroleum ether 2:1. Yield 306 mg, 85%. $[\alpha]_D$ 23 °C = +63.2°, (c = 2.5, $CHCl_3$).

^1H NMR (500 MHz, Me_2SO) 1.20, 1.32 (6 H, 2 s, $C(CH_3)_2$), 3.21 (3 H, s, ribose-OMe), 3.26 (1 H, dd, J = 7.2, 8.6 Hz, H-Ins), 3.46−3.58 (3 H, m, CH_2OBn, H-5-ribose, H-2 or H-3-Ins), 3.66 (1 H, dt, J = 2.2, 4.7 Hz, H-2 or H-3-Ins, D_2O exch.), 3.73, 3,73 (6 H, 2 s, CH_2PhOMe), 3.77 (1 H, dd, J = 2.1, 5.1 Hz, H-Ins), 3.87 (1 H, d, J = 4.7 Hz, H-2-ribose), 4.02 (1 H, m, H-4-ribose), 4.13 (1 H, dd, J = 6.8, 8.5 Hz, H-Ins), 4.20−4.25 (2 H, m, H-Ins and H-ribose), 4.51−4.67 (6 H, m, CH_2Ph, 2 × CH_2PhOMe), 4.85 (1 H, s, H-1-ribose), 4.97 (1 H, d, J = 4.7 Hz, D_2O exch., Ins-OH), 5.15 (1 H, d, J = 5.1 Hz, D_2O exch., Ins-OH), 6.87−6.89 (4 H, m, 2 × CH_2PhOMe), 7.24−7.32 (9 H, m, CH_2Ph, 2 × CH_2PhOMe).

^{13}C NMR (125 MHz, Me_2SO) 25.47, 27.71 (2 q, $C(CH_3)_2$), 54.28, 55.02, 55.02 (3 q, 2 × CH_2PhOMe, ribose-OMe), 71.14, 71.16, 71.71, 72.19 (4 t, CH_2Ph, CH_2PhOMe, CH_2OBn), 73.08, 74.04, 76.74, 77.85 (2 carbon signals), 78.38, 79.07, 80.04, 83.52, 105.74 (10 × -C-H ring carbons for inositol and ribose), 108.31 (C_q, $C(Me)_2$), 113.37, 113.59 (C-H, 2 × CH_2PhOMe), 127.28 (2 carbon signals), 127.32, 128.17, 129.00, 129.72 (d, C-H, CH_2Ph, CH_2PhOMe), 129.95, 130.98, 138.39 (C_q, s, CH_2Ph, CH_2PhOMe), 158.47, 158.47 (C_q, s, CH_2PhOMe).

M/z $C_{38}H_{48}NaO_{12}$ $[M + Na]^+$ expected 719.3038; found 719.3009.

(3a*S*,4*R*,5*R*,6*R*,7*S*,7a*R*)-6-(Benzyloxy)-4-(((3*R*,4*R*,5*R*)-2-((Benzyloxy)methyl)-5-methoxy-4-((4-methoxybenzyl)oxy)-tetrahydrofuran-3-yl)oxy)-7-((4-methoxybenzyl)oxy)-2,2-dimethylhexahydrobenzo[*d*][1,3]dioxol-5-ol (15) and (3a*R*,4*S*,5*R*,6*R*,7*R*,7a*S*)-6-(Benzyloxy)-7-(((3*R*,4*R*,5*R*)-2-((Benzyloxy)methyl)-5-methoxy-4-((4-methoxybenzyl)oxy)-tetrahydrofuran-3-yl)oxy)-4-((4-methoxybenzyl)oxy)-2,2-dimethylhexahydrobenzo[*d*][1,3]dioxol-5-ol (16). The diol (**14**, 419 mg, 0.60 mmol) and dibutyltin oxide (180 mg, 0.72 mmol) in toluene (100 mL) were heated at reflux temperature overnight for 18 h with the Dean−Stark apparatus with the removal of water. The reaction mixture was cooled and the solvents were evaporated off to give a glassy residue, which was dried overnight. Cesium fluoride (327 mg, 2.16 mmol), dry dimethylformamide (DMF) (10 mL), and benzyl bromide (240 μL, 2.0 mmol) were added to the mixture, which was stirred overnight (18 h). TLC (EtOAc/petrol, 1:1) showed two products R_f = 0.50 and R_f = 0.42. The solvents were evaporated under reduced pressure, the residue was partitioned between EtOAc and water (20 mL of each), and the organic phase was stirred with sodium hydrogen carbonate solution (20 mL) for 30 min. The resulting milky organic layer was filtered over a bed of celite, dried, and the solvent was evaporated. The resulting residue was purified by flash chromatography (EtOAc/petroleum ether, 2:3) to give the title compound as a glass (122 mg, 30.5%) (of consumed compound), (upper spot) together with the lower R_f product (124 mg, 31%) and 66 mg of starting material, thus 353 mg is used up. Yields were based upon the benzylated compound.

3-*O*-Benzyl Diastereoisomer (15). ^1H NMR (400 MHz, CD_3CN) 1.35, 1.47 (6 H, 2 s, $C(CH_3)_2$), 3.28 (3 H, s, ribose-OMe), 3.49−3.55 (2 H, m, H-Ins), 3.60−3.71 (3 H, m, -CH_2OBn, H-Ins), 3,79, 3.84 (6 H, 2 s, 2 × CH_2PhOMe), 3.87−3.92 (2 H, m, 2 × H-Ins), 4.00 (1 H, dd, J = 1.3, 4.9 Hz, H-2-ribose), 4.15 (1 H, ddd, J = 3.9, 5.8, 6.8 Hz, H-4-ribose), 4.22 (1 H, m, H-Ins), 4.28 (1 H, dd, J = 4.8, 6.7 Hz, H-3-ribose), 4.33 (1 H, dd, J = 4.7, 6.5 Hz, H-Ins), 4.58−4.78 (8 H, CH_2Ph, CH_2PhOMe), 5.05 (1 H, d, J = 1.2 Hz, H-1-ribose), 6.92 (2 H, d, J = 8.9 Hz, CH_2PhOMe), 6.93 (2 H, d, J = 8.9 Hz, CH_2PhOMe), 7.32 (2 H, d, J = 8.9 Hz, CH_2PhOMe), 7.34−7.43 (12 H, m, 2 × CH_2Ph, CH_2PhOMe).

^{13}C NMR (100 MHz, CD_3CN) 25.96, 28.17 (2 q, $C(CH_3)_2$), 55.39 (2 carbon signals), 55.83 (3 q, 2 × CH_2PhOMe, ribose-OMe), 72.41, 72.46, 73.73, 73.77, 74.11 (5t, CH_2Ph, CH_2PhOMe, CH_2OBn), 72.23, 76.61, 79.44, 79.68, 79.90, 80.57, 81.73, 82.78, 83.14, 106.95 (10 × -C-H ring carbons for inositol and ribose), 110.08 (C_q, $C(Me)_2$), 114.44, 114.70 (C-H, 2 × CH_2PhOMe), 128.37, 128.47, 128.58, 128.81, 129.15, 129.30, 130.40, 131.05 (d, C-H, CH_2Ph, CH_2PhOMe), 130.50, 132.08, 139.63, 140.00 (C_q, s, CH_2Ph, CH_2PhOMe), 160.09, 160.48 (C_q, s, CH_2PhOMe). M/z $C_{45}H_{54}NaO_{12}$ $[M + Na]^+$ expected 809.3507; found 809.3534. 3-*O*-Benzyl diastereoisomer: $[\alpha]_D$ 20 °C = +61.8°, (c = 2.48, $CHCl_3$).

2-*O*-Benzyl Derivative (16). ^1H NMR (500 MHz, $CDCl_3$) 1.28, 1.43 (6 H, 2 s, $C(CH_3)_2$), 3.28 (3 H, s, ribose-OMe), 3.40 (1 H, dd, J = 6.9, 8.9 Hz, H-4-Ins), 3.56 (2 H, d, J = 5.0 Hz, -CH_2OBn), 3.62 (1 H, dd, J = 2.6, 8.0 Hz, H-2-Ins), 3.73, 3.79 (6 H, 2 s, 2 × CH_2PhOMe), 3.85 (1 H, dd, J = 1.3, 8.3 Hz, H-2-ribose), 3.98 (1 H, dt, J = 1.8, 8.3 Hz, H-3-Ins), 4.08 (1 H, t, J = 3.2 Hz, H-1-Ins), 4.19−4.22 (1 H, m, H-4-ribose), 4.24−4.31 (3 H, m, H-3-ribose, H-6-Ins, H-5-Ins), 4.44−4.85 (8 H, m, 2 × CH_2Ph, 2 × CH_2PhOMe), 4.77 (1 H, d, J = 1.3 Hz), 6.76 (2 H, d, J = 8.7 Hz, CH_2PhOMe), 6.86 (2 H, d, J = 8.7 Hz, CH_2PhOMe), 7.15 (2 H, d, J = 8.9 Hz, CH_2PhOMe), 7.25−7.32 (12 H, m, 2 × CH_2Ph, CH_2PhOMe).

^{13}C NMR (125 MHz, $CDCl_3$) 25.92, 27.93 (2 q, $C(CH_3)_2$), 55.13, 55.20, 55.25 (3 q, 2 × CH_2PhOMe, ribose-OMe), 71.06, 72.12, 72.75, 72.20, 73.32 (5t, CH_2Ph, CH_2PhOMe, CH_2OBn), 71.47, 76.05, 76.56, 79.02, 79.94, 80.27, 80.45, 80.91, 83.41, 106.47 (10 × -C-H ring carbons for inositol and ribose), 109.39 (C_q, $C(Me)_2$), 113.68, 113.74 (C-H, 2 × CH_2PhOMe), 127.54, 127.55, 127.66, 127.86, 128.34, 128.35, 129.53, 129.55 (d, C-H, CH_2Ph, CH_2PhOMe), 130.11, 130.75, 138.10, 138.16 (C_q, s, CH_2Ph, CH_2PhOMe), 159.12, 159.15 (C_q, s, CH_2PhOMe). M/z $C_{45}H_{54}NaO_{12}$ $[M + Na]^+$ expected 809.3507; found 809.3526. 2-*O*-Benzyl diastereoisomer: $[\alpha]_D$ 20 °C = +19.1°, (c = 2.44, $CHCl_3$).

(3a*R*,4*S*,5*S*,6*R*,7*R*,7a*S*)-6-(Benzyloxy)-7-(((3*S*,4*R*,5*R*)-2-((benzyloxy)methyl)-4-hydroxy-5-methoxytetrahydrofuran-3-yl)oxy)-2,2-dimethylhexahydrobenzo[*d*][1,3]dioxole-4,5-diol (17). A mixture of the 2-*O*-benzyl derivative (**16**, 184 mg, 0.234 mmol) and DDQ (188 mg, 0.825 mmol) was stirred in dichloromethane (9.5 mL) and water (0.5 mL) for 1 h after which a salmon-colored precipitate was observed. The reaction was diluted with dichloromethane (40 mL), and the precipitate was filtered off and washed with 10% sodium sulfite solution (2 × 20 mL), then washed with sodium hydrogen carbonate solution (20 mL) and water (20 mL), dried, filtered, and the dichloromethane was evaporated to give an oil. The oily residue was chromatographed on silica gel using a gradient of petrol to 70% ethyl acetate to give the title compound **17**; yield (80 mg, 63%); R_f = 0.42 (ethyl acetate).

^1H NMR (500 MHz, $CDCl_3$) 1.25 1.43 (6 H, 2 s, $C(CH_3)_2$), 2.66 (1 H, d, J = 3.4 Hz, D_2O, exch. Ins-3-OH), 2.88 (1 H, d, J = 4.5 Hz, D_2O, exch. Ins-4-OH), 3.32 (3 H, s, ribose-OMe), 3.51−3.63 (4 H, m, CH_2OBn, H-5-ribose, H-2 or H-3-Ins), 3.86 (1 H, t, J = 2.9 Hz, H-1 or H-6-Ins), 3.89 (1 H, dt, J = 3.1, 8.8 Hz, D_2O exch. J = 8.8 Hz, H-3-

https://dx.doi.org/10.1021/acs.jmedchem.9b01986
J. Med. Chem. 2020, 63, 3238−3251

Ins), 4.02−4.04 (2 H, m, Ins and/or H-ribose), 4.10−4.16 (3 H, H-Ins and/or H-ribose, ribose-2-OH, D_2O exch.), 4.18 (1 H, dd, J = 2.8, 5.4 Hz, H-Ins or H-ribose), 7.26−7.38 (10 H, m, 2 × CH_2Ph).

^{13}C NMR (125 MHz, $CDCl_3$) 25.72, 27.83 (2 q, $C(CH_3)_2$), 54.92 (ribose-O*Me*), 71.81, 73.45, 74.10 (3t, CH_2Ph, CH_2OBn), 71.81, 72.51, 74.37, 75.77, 76.11, 78.39 (2 carbon signals), 79.20, 81.35, 108.01 (10 × -*C*-H ring carbons for inositol and ribose), 110.89 (C_q, $C(Me)_2$), 127.61, 127.72, 128.42, 128.71 (d, *C*-H, CH_2Ph), 136.83, 137.90 (C_q, s, CH_2Ph). M/z $C_{29}H_{38}NaO_{10}$ $[M + Na]^+$ expected 569.2357; found 569.2366. $[\alpha]_D$ 22 °C = + 23.5°, (c = 1.1, $CHCl_3$).

Tetrabenzyl ((3a*S*,4*R*,6*S*,7*R*,7a*S*)-6-(Benzyloxy)-7-(((3*R*,4*R*,5*R*)-2-((benzyloxy)methyl)-4-((bis(benzyloxy)-phosphoryl)oxy)-5-methoxytetrahydrofuran-3-yl)oxy)-2,2-dimethylhexahydrobenzo[*d*][1,3]dioxole-4,5-diyl) Bis-(phosphate) (19). A mixture of bis(benzyloxy)-diisopropylaminophosphine (0.345 g, 1 mmol) and 1*H*-tetrazole (0.21 g, 3 mmol) in dry $CDCl_3$ (3 mL) was stirred for 15 min at room temperature. The phosphitylating complex was added to the triol (**17**, 65 mg, 0.119 mmol) in $CDCl_3$ (2 mL) and stirred for 30 min to give the P(III) intermediate (**18**). Solid *m*CPBA (345 mg, 2.0 mmol) was added to the cooled solution using a dry ice−acetone bath, and the P(III) intermediate was oxidized and stirred for a further 30 min. The solution was diluted with EtOAc (20 mL) and washed with 10% aqueous sodium sulfite solution (2 × 20 mL). The organic layer was dried ($MgSO_4$), and the product was purified by flash chromatography using a gradient of petroleum ether ethyl acetate 100% petroleum ether to (EtOAc/petroleum ether, 2:1), to give the trisphosphate (**19**, 114 mg, 72%).

^1H NMR (500 MHz, CD_3CN) 1.25 1.43 (6 H, 2 s, $C(CH_3)_2$), 3.55−3.69 (2 H, ABX, J = 10.7, 3.5, 5.4 Hz, H-5-ribose), 4.10−4.13 (1 H, m, obscured, H-4-ribose), 4.14 (1 H, dd, J = 2.4, 6.5 Hz, H-Ins), 4.24 (1 H, t, J = 2.2 Hz, H-1-Ins), 4.38 (1 H, dd, J = 6.9, 9.35 Hz, H-Ins), 4.46 (1 H, t, J = 6.5 Hz, H-Ins or H-ribose), 4.46 (1 H, dd, J = 2.1, 7.3 Hz, H-Ins or H-ribose), 4.53−4.69 (7 H, m, H-2-ribose, H-3-Ins, H-4-Ins, 2 × CH_2Ph), 4.83 (1 H, s, H-1-ribose), 4.96−5.10 (12 H, 3 × P(O)O(CH_2Ph)$_2$), 7.23−7.37 (40 H, 3 × P(O)O(CH_2Ph)$_2$, 2 × CH_2Ph). ^{31}P NMR (202.4 MHz, CD_3CN) −1.43, −1.60, −1.77.

^{13}C NMR (125.7 MHz, CD_3CN) 25.72, 27.93 (2 q, $C(CH_3)_2$), 55.44 (ribose-O*Me*), 69.91 [(P-coupled, J = 5.6), 70.17 (P-coupled, J = 5.8 Hz), 70.29 (P-coupled J = 5.7), 5.37 (P-coupled, J = 5.7 Hz), 70.49 (P-coupled, J = 5.8 Hz, 2 carbon signals), (3 × P(O)-(OCH$_2$Ph)$_2$)], 71.90, 73.60, 73.80 (t, 2 × CH_2Ph, CH_2OBn), 76.43, 77.77, 78.25, 78.33 [(P-coupled, J = 4.6 Hz), 78.61 (P-coupled, J = 5.2 Hz), 79.27 (P-coupled, J = 5.3 Hz), 80.98, 81.07, 81.82 (P-coupled, J = 5.8, 7.6 Hz)], 107.04 (P-coupled, J = 4.6 Hz), 111.47 (C_q, $C(Me)_2$), 128.46, 128.48, 128.51, 128.52, 128.84, 129.01, 129.03, 129.15, 129.20, 129.25, 129.30, 129.39, 129.42, 129.45, 129.47, 129.49, 129.52, 129.56 (d, *C*-H, CH_2Ph), 137.02, 137.04, 137.07, 137.09, 137.13, 137.26, 137.33, 137.48, 137.54, 139.13, 139.53 (C_q, s, CH_2Ph). M/z $C_{71}H_{77}NaO_{19}P_3$ $[M + Na]^+$ expected 1349.4164; found 1349.4121. $[\alpha]_D$ 23 °C = + 20.7°, (c = 1.9, $CHCl_3$).

(2*R*,3*S*,4*R*,5*S*,6*S*)-3,4,6-Trihydroxy-5-(((3*R*,4*R*,5*R*)-2-(hydroxy-methyl)-5-methoxy-4-(phosphonatooxy)tetrahydrofuran-3-yl)oxy)cyclohexane-1,2-diyl bis(phosphate) (10) [D-*chiro*-Inositol Ribophostin (10)]. The phosphorylated compound (**19**, 90 mg, 67.8 μmoles) was dissolved in MeOH (4 mL), and water (1 mL) was added. Palladium hydroxide (10, 15 mg) was stirred vigorously in the presence of a balloon of hydrogen for 19.5 h. About one-third (by volume) was removed and filtered, then two drops of triethylamine were added to form the salt and ^1H NMR was conducted. At this stage, the removal of the isopropylidene was incomplete (about a third was removed). One-third of the sample was evaporated to dryness and acidified using 80% acetic acid in D_2O (5.0 mL in total), then stirred for 3 h. The NMR results indicated that it was incomplete and was stirred in 80% acetic acid for a further 6 h and then for another 2 h. The remaining compound was then left under stirring for about 1 week. After this time, methanol was removed and triethylamine was added. NMR results indicated that the isopropylidene group had been removed. The remaining compound was purified over Q-Sepharose ion-exchange resin using a gradient of 0−2 M TEAB buffer. The compound eluted between 1.1 and 1.4 M buffer and then on RP18 resin. Yield (28.9 μmoles, 42.6%).

^1H NMR (400 MHz, MeOD) 3.41 (s, ribose-O*Me*), 3.63 (1 H, dd, J = 6 Hz, 12 Hz, H-5a-ribose), 3.75 (1 H, dd, J = 3.6 Hz, 11.6 Hz, H-5b-ribose), 3.90 (1 H, dd, J = 3.2 Hz, 9.6 Hz, H-5-Ins), 3.98−4.05 (2 H, m, H-2-Ins, H-4-ribose), 4.09 (1 H, t, J = 3.6 Hz, H-1 or H-6-Ins), 4.17−4.20 (br m, H-3-ribose), 4.31 (1 H, app q, J = 8.8 Hz, J = 9.2 Hz, H-3-Ins), 4.48 (1 H, app q, J = 8.8 Hz, J = 9.2 Hz, H-4-Ins), 4.65 (1 H, dd, J = 4.4 Hz, H-2-ribose), 5.14 (s, H-1-ribose); 13 C NMR (125.7 MHz, MeOD) 52.25 (ribose-O*Me*), 64.73 ($HOCH_2$-ribose), 70.68 (C-6-Ins), 72.10 (C-2-Ins), 72.85 (C-5-Ins), 77.36 (C-2-ribose), 78.24 (C-4-Ins), 78.59 (C-3-Ins), 81.75 (C-3-Ribose), 82.37 (C-1-Ins), 83.13 (C-4-ribose), 108.69 (C-1-ribose); ^{31}P NMR (202 MHz, MeOD) +2.56, +1.93, +0.82; M/z $C_{12}H_{24}O_{19}P_3$ $[M - H]^-$ expected 565.0130; found 565.0136.

D-3-*O*-1*S*-(−)-Camphanoyl-1,2:4,5-di-*O*-isopropylidene-*myo*-inositol (21). The upper diastereoisomer (**20**, 560.6 mg, 1.0 mmol) and DDQ (454 mg, 2 mmol) in dichloromethane 0.5 M phosphate buffer pH 7.4 (20 mL, 19:1) were stirred at room temperature overnight to give a deep green solution. The solution was diluted with dichloromethane (100 mL), and the pink-red precipitate that formed overnight was filtered off. The organic solution was then washed with a 10% solution of sodium hydrogen carbonate (2 × 100 mL) and water (100 mL). The organic layer was dried, filtered, and evaporated to give the crude product with R_f = 0.24 (ethyl acetate/petroleum ether, 1:1) and R_f of starting material = 0.54. The crude product was purified by flash chromatography (ethyl acetate/petroleum ether, 1:1 to ethyl acetate) to give the alcohol as a solid in 63% yield (279 mg). The compound was recrystallized from *t*-butylmethyl ether−hexane. $[\alpha]_D$ + 24° at temp = 22 °C, c = 0.50 ($CHCl_3$), mp = 223−226 °C. ^1H NMR (400 MHz, $CDCl_3$) 0.98 (3 H, s, CH_3- camphanate), 1.05 (3 H, s, CH_3- camphanate), 1.11 (3 H, s, CH_3-, camphanate), 1.28, 1.43 (6 H, 2 s, C-$(CH_3)_2$, isopropylidene), 1.45, 1.49 (6 H, 2 s, C-$(CH_3)_2$, isopropylidene), 1.65−1.72 (1 H, m, -*CH*- of -CH_2-, camphanate), 1.88−1.95 (1 H, m, -*CH*- of -CH_2-, camphanate), 2.04−2.10 (1 H, m, -*CH*- of -CH_2-, camphanate), 2.44−2.51 (1 H, m, -*CH*- of -CH_2-, camphanate), 2.53 (1 H, d, J = 2.6 Hz, D_2O exch. Ins-O*H*), 3.40 (1 H, dd, J = 9.5, 10.7 Hz, H-5), 3.88−3.93 (1 H, br ddd, 2.3, 6.5, 9.1 Hz, D_2O exch. J = 6.5, 10.7 Hz, H-6), 4.05 (1 H, dd, J = 9.5 Hz, 10.4 Hz, H-4), 4.08 (1 H, t, J = 5.8 Hz, H-1), 4.63 (1 H, t, J = 4.8 Hz, H-2), 5.20 (1 H, dd, J = 4.4, 10.5 Hz, H-3).

^{13}C NMR (100 MHz, $CDCl_3$) 9.74, 16.49, 16.65 (3 q, -CH_3, camphanate), 25.74, 26.85, 26.94, 28.10 (4 q, 2 × $C(CH_3)_2$), 28.98, 30.58 (2 t, 2 × -CH_2-, camphanate), 54.71, 54.90 (2 s, C_q, camphanate), 72.10, 74.43, 74.49, 74.63, 78.14, 81.90 (6 d, 6 × inositol ring carbons), 91.02 (s, C_q, camphanate), 110.33, 112.99 (2 s, C_q, $C(CH_3)_2$), 167.14 (s, C_q, (O-C=O), camphanate), 178.11 (s, C_q, C=O, camphanate). $C_{22}H_{32}O_9$, Expected: C = 59.99, H = 7.32; Found: C = 60.0, H = 7.42. M/z $C_{22}H_{32}NaO_9$, Expected: 463.1939; Found 463.1950.

D-(−)-1,2:4,5-Di-*O*-isopropylidene-*myo*-inositol (22). A mixture of D-3-*O*-1*S*-(−)-Camphanoyl-1,2:4,5-di-*O*-isopropylidene-*myo*-inositol (**21**, 237 mg, 0.538 mmol) and MeOH (50 mL) was heated under reflux in the presence of NaOH (73 mg, 1.82 mmol) for 30 min. The solvent was further diluted with MeOH (50 mL), and the solution was neutralized by bubbling carbon dioxide through it. Water (10 mL) was added, and the solvents were evaporated off to give a solid. Extraction of the product (CH_2Cl_2) gave the (EtOAc-CH_2Cl_2, R_f = 0.20) purified product as a white solid (115 mg, 82%) from EtOAc. $[\alpha]_D$ = −23°, temperature = 21 °C, c = 0.50 in CH_3CN, Lit. + 22° (c = 1.08, MeCN)[36] (for opposite enantiomer). Lit. −22° (c = 1, MeCN)[37] Lit. −21.7° (c = 0.46, MeCN);[38] mp 157−159 °C; Lit.[36] mp = 159−161 °C.

^1H NMR (400 MHz, $CDCl_3$) 1.36, 1.44, 1.47, 1.52 (12 H, 2 × $C(CH_3)_2$, isopropylidene), 2.56 (1 H, d, J = 8.6 Hz, Ins-3-OH, D_2O, exch.), 2.80 (1 H, d, J = 3.0 Hz, Ins-6-OH, D_2O, exch.), 3.31 (1 H, dd, J = 9.4, 10.7 Hz, H-5), 3.82 (1 H, t, J = 9.6 Hz, H-4), 3.88 (1 H, ddd, J = 3.0, 6.5, 10.7 Hz, D_2O exch. dd, J = 6.4, 10.7 Hz, H-6), 4.02 (1 H,

https://dx.doi.org/10.1021/acs.jmedchem.9b01986
J. Med. Chem. 2020, 63, 3238−3251

ddd, 4.5, 8.6, 10.6 Hz, D_2O exch. dd, J = 4.5, 10.1 Hz, H-3), 4.06 (1 H, dd, J = 5.8, 6.4 Hz, H-1), 4.46 (1 H, t, J = 4.8 Hz, H-2).

^{13}C NMR (100 MHz, $CDCl_3$) 25.86, 26.89, 26.90, 28.08 (4 q, 2 × $C(CH_3)_2$, isopropylidene), 69.80, 74.82, 77.59, 77.98, 78.03, 81.84 (6 d, inositol ring carbons), 110.29, 112,72 (2 s, C_q, 2 × $C(CH_3)_2$, isopropylidene).

■ ASSOCIATED CONTENT

Supporting Information

The Supporting Information is available free of charge at https://pubs.acs.org/doi/10.1021/acs.jmedchem.9b01986.

Spectral data including ^1H NMR, ^{31}P NMR, and ^{13}C NMR for compounds, including final compound (PDF)

Molecular formula strings (CSV)

■ AUTHOR INFORMATION

Corresponding Author

Barry V. L. Potter − *Drug Discovery & Medicinal Chemistry, Department of Pharmacology, University of Oxford, Oxford OX1 3QT, United Kingdom;* orcid.org/0000-0003-3255-9135; Email: barry.potter@pharm.ox.ac.uk

Authors

Stephen J. Mills − *Drug Discovery & Medicinal Chemistry, Department of Pharmacology, University of Oxford, Oxford OX1 3QT, United Kingdom*

Ana M. Rossi − *Department of Pharmacology, University of Cambridge, Cambridge CB2 1PD, United Kingdom*

Vera Konieczny − *Department of Pharmacology, University of Cambridge, Cambridge CB2 1PD, United Kingdom*

Daniel Bakowski − *Centre of Integrative Physiology, Department of Physiology, Anatomy and Genetics, University of Oxford, Oxford OX1 3PT, United Kingdom*

Colin W. Taylor − *Department of Pharmacology, University of Cambridge, Cambridge CB2 1PD, United Kingdom*

Complete contact information is available at: https://pubs.acs.org/10.1021/acs.jmedchem.9b01986

Author Contributions

The manuscript was written by S.J.M. and B.V.L.P. with contributions from all authors, who approved the final version.

Notes

The authors declare no competing financial interest.

■ ACKNOWLEDGMENTS

This work was supported by the Wellcome Trust. B.V.L.P. and C.W.T. are Wellcome Trust Senior Investigators (grant Nos. 101010 and 101844, respectively). A.M.R. is a Fellow at Queens' College, Cambridge. The authors thank Drs. Xiangdong Su and Wolfgang Dohle for a sample of authentic **4** and Dr A. M. Riley for useful discussions during this work.

■ ABBREVIATIONS

DDQ, 2,3-dichloro-5,6-dicyano-1,4-benzoquinone; HMPA, hexamethyl-phosphoramide; Ins(1,4,5)P_3, D-*myo*-inositol trisphosphate; Ins(1,4,5)P_3R, D-*myo*-inositol trisphosphate receptor; THF, tetrahydrofuran; HEK, human embryonic kidney; SEM, standard error of mean; IBC, inositol binding core; RBL, rat basophilic leukemic; TEAB, triethylammonium bicarbonate

■ REFERENCES

(1) Bosanac, I.; Alattia, J.-R.; Mal, T. K.; Chan, J.; Talarico, S.; Tong, F. K.; Tong, K. I.; Yoshikawa, F.; Furuichi, T.; Iwai, M.; Michikawa, T.; Mikoshiba, K.; Ikura, M. Structure of the inositol 1,4,5-trisphosphate receptor binding core in complex with its ligand. *Nature* **2002**, *420*, 696−700.

(2) Fan, G.; Baker, M. R.; Wang, Z.; Seryshev, A. B.; Ludtke, S. J.; Baker, M. L.; Serysheva, I. I. Cryo-EM reveals ligand induced allostery underlying $InsP_3R$ channel gating. *Cell Res.* **2018**, *28*, 1158−1170.

(3) Paknejad, N.; Hite, R. K. Structural basis for the regulation of inositol trisphosphate receptors by Ca^{2+} and IP_3. *Nat. Struct. Mol. Biol.* **2018**, *25*, 660−668.

(4) Rossi, A. M.; Taylor, C. W. IP_3 receptors—lessons from analyses *ex cellula*. *J. Cell. Sci.* **2019**, *132*, No. jcs222463.

(5) Potter, B. V. L.; Lampe, D. Chemistry of inositol lipid mediated cellular signaling. *Angew. Chem., Int. Ed.* **1995**, *34*, 1933−1972.

(6) Swarbrick, J. M.; Riley, A. M.; Mills, S. J.; Potter, B. V. L. Designer small molecules to target calcium signalling. *Biochem. Soc. Trans.* **2015**, *43*, 417−425.

(7) Thomas, M. P.; Mills, S. J.; Potter, B. V. L. The "other" inositols and their phosphates: synthesis, biology and medicine (with recent advances in myo-inositol chemistry). *Angew. Chem., Int. Ed.* **2016**, *55*, 1614−1650.

(8) Takahashi, M.; Kagasaki, T.; Hosoya, T.; Takahashi, S. Adenophostins A and B: potent agonists of inositol-1,4,5-trisphosphate receptor produced by *Penicillium brevicompactum*. *J. Antibiot.* **1993**, *46*, 1643−1647.

(9) Takahashi, M.; Tanzawa, K.; Takahashi, S. Adenophostins, newly discovered metabolites of *Penicillium brevicompactum*, act as potent agonists of the inositol 1,4,5-trisphosphate receptor. *J. Biol. Chem.* **1994**, *269*, 369−372.

(10) Takahashi, S.; Kinoshita, T.; Takahashi, M. Adenophostins A and B: potent agonists of the inositol-1,4,5-trisphosphate receptor produced by *Penicillium brevicompactum*. structure elucidation. *J. Antibiot.* **1994**, *47*, 95−100.

(11) Saleem, H.; Tovey, S. C.; Riley, A. M.; Potter, B. V. L.; Taylor, C. W. Stimulation of inositol 1,4,5-trisphosphate (IP_3) receptor subtypes by adenophostin A and its analogues. *PLoS One* **2013**, *8*, No. e58027.

(12) Rossi, A. M.; Sureshan, K. M.; Riley, A. M.; Potter, B. V. L.; Taylor, C. W. Selective determinants of inositol 1,4,5-trisphosphate and adenophostin A interactions with type 1 inositol 1,4,5-trisphosphate receptors. *Br. J. Pharmacol.* **2010**, *161*, 1070−1085.

(13) Sureshan, K. M.; Riley, A. M.; Thomas, M. P.; Tovey, S. C.; Taylor, C. W.; Potter, B. V. L. Contribution of phosphates and adenine to the potency of adenophostins at the IP_3 receptor: synthesis of all possible bisphosphates of adenophostin A. *J. Med. Chem.* **2012**, *55*, 1706−2120.

(14) Mochizuki, T.; Kondo, Y.; Abe, H.; Tovey, S. C.; Dedos, S. G.; Taylor, C. W.; Paul, M.; Potter, B. V. L.; Matsuda, A.; Shuto, S. Synthesis of adenophostin A analogues conjugating an aromatic group at the 5′-position as potent IP_3 receptor ligands. *J. Med. Chem.* **2006**, *49*, 5750−5758.

(15) Mochizuki, T.; Tanimura, A.; Nezu, A.; Ito, M.; Abe, H.; Ito, Y.; Arisawa, M.; Shuto, S. Design and synthesis of indole derivatives of adenophostin A. A entry into subtype-selective IP_3 receptor ligands. *Tetrahedron Lett.* **2010**, *51*, 977−979.

(16) Vibhute, A. M.; Konieczny, V.; Taylor, C. W.; Sureshan, K. M. Triazolophostins: a library of novel and potent agonists of IP_3 receptors. *Org. Biomol. Chem.* **2015**, *13*, 6698−6910.

(17) Vibhute, A. M.; Pushpanandan, P.; Varghese, M.; Konieczny, V.; Taylor, C. W.; Sureshan, K. M. Synthesis of dimeric analogs of adenophostin A that potently evoke Ca^{2+} release through IP_3 receptors. *RSC Adv.* **2016**, *6*, 86346−86351.

(18) Rossi, A. M.; Riley, A. M.; Potter, B. V. L.; Taylor, C. W. Adenophostins: high-affinity agonists of IP_3 receptors. *Curr. Top. Membr.* **2010**, *66*, 209−233.

(19) Correa, V. A.; Riley, A. M.; Shuto, S.; Horne, G.; Nerou, E. P.; Marwood, R. D.; Potter, B. V. L.; Taylor, C. W. Structural

determinants of adenophostin A activity at inositol trisphosphate receptors. *Mol. Pharmacol.* **2001**, *59*, 1206−1215.
(20) Dohle, W.; Su, X.; Mills, S. J.; Rossi, A. M.; Taylor, C. W.; Potter, B. V. L. A synthetic cyclitol-nucleoside conjugate polyphosphate is a highly potent second messenger mimic. *Chem. Sci.* **2019**, *10*, 5382−5390.
(21) Rosenberg, H. J. A.; Riley, A. M.; Laude, A. J.; Taylor, C. W.; Potter, B. V. L. Synthesis and Ca^{2+} mobilising activity of purine-modified mimics of adenophostin A: a model for the adenophostin-Ins(1,4,5)P_3 receptor interaction. *J. Med. Chem.* **2003**, *46*, 4860−4871.
(22) Sureshan, K. M.; Riley, A. M.; Rossi, A. M.; Tovey, S. C.; Dedos, S. G.; Taylor, C. W.; Potter, B. V. L. Activation of IP_3 receptors by synthetic bisphosphate ligands. *Chem. Commun.* **2009**, *45*, 1204−1206.
(23) Nerou, E. P.; Riley, A. M.; Potter, B. V. L.; Taylor, C. W. Selective recognition of inositol phosphates by subtypes of the inositol trisphosphate receptor. *Biochem. J.* **2001**, *355*, 59−69.
(24) Chrètien, F.; Moitessier, N.; Roussel, F.; Mauger, J.-P.; Chapleur, Y. Carbohydrate based mimics of D-*myo*-inositol 1,4,5-trisphosphate. *Curr. Org. Chem.* **2000**, *4*, 513−534.
(25) Hotoda, H.; Murayama, K.; Miyamoto, S.; Iwata, Y.; Takahashi, M.; Kawase, Y.; Tanzawa, K.; Kaneko, M. Adenophostin, a very potent Ca^{2+} inducer at the d-*myo*-inositol 1,4,5-trisphosphate receptor. *Biochemistry* **1999**, *38*, 9234−9241.
(26) Safrany, S. T.; Wojcikiewicz, R. J. H.; Strupish, J.; Nahorski, S. R.; Dubreuil, D.; Chleophax, J.; Gero, S. D.; Potter, B. V. L. Interaction of synthetic D-6-deoxy-*myo*-inositol 1,4,5-trisphosphate with the Ca^{2+}-releasing D-*myo*-1,4,5-trisphosphate receptor and the metabolic enzymes 5-phosphatase and 3-kinase. *FEBS Lett.* **1991**, *278*, 252−256.
(27) Jenkins, D. J.; Potter, B. V. L. (2-Hydroxyethyl)-α-d-glucopyranoside 2′,3,4-trisphosphate: synthesis of a second messenger mimic related to adenophostin A. *J. Chem. Soc., Chem. Commun.* **1995**, 1169−1170.
(28) Jenkins, D. J.; Potter, B. V. L. A Ca^{2+} mobilising carbohydrate-based polyphosphate: synthesis of 2-hydroxyethyl-α-D-glucopyranoside 2′,3,4-trisphosphate. *Carbohydr. Res.* **1996**, *287*, 169−182.
(29) Wilcox, R. A.; Erneux, C.; Primrose, W. U.; Gigg, R.; Nahorski, S. R. 2-Hydroxyethyl α-D-glucopyranoside 2,3′,4′-trisphosphate: a novel metabolically resistant adenophostin A and *myo*-inositol 1,4,5-trisphosphate analogue potently interacts with the *myo*-inositol 1,4,5-trisphosphate receptor. *Biochem. Soc. Trans.* **1995**, *23*, 420S.
(30) Rosenberg, H. J.; Riley, A. M.; Marwood, R. D.; Correa, V.; Taylor, C. W.; Potter, B. V. L. Xylopyranoside-based agonists of D-*myo*-inositol 1,4,5-trisphosphate receptors: synthesis and effect of stereochemistry on biological activity. *Carbohydr. Res.* **2001**, *332*, 53−56.
(31) Jenkins, D. J.; Marwood, R. D.; Potter, B. V. L. A disaccharide polyphosphate mimic of 1D-*myo*-inositol 1,4,5-trisphosphate. *Chem. Commun.* **1997**, 449−450.
(32) Mills, S. J.; Potter, B. V. L. Synthesis of D- and L-*myo*-inositol 1,4,6-trisphosphate, regioisomers of a ubiquitous second messenger. *J. Org. Chem.* **1996**, *61*, 8980−8987.
(33) Hamblin, M. R.; Potter, B. V. L.; Gigg, R. Bis-phosphorylation of a *vic*-diol: synthesis of *myo*-inositol 4,5-bisphosphate. *J. Chem. Soc., Chem. Commun.* **1987**, 626−627.
(34) Briggs, A. J. A modification of the Bell−Doisy phosphate method. *J. Biol. Chem.* **1922**, *53*, 13−16.
(35) Lampe, D.; Liu, C.; Potter, B. V. L. Synthesis of selective non-Ca^{2+} mobilizing inhibitors of D-*myo*-inositol 1,4,5-trisphosphate 5-phosphatase. *J. Med. Chem.* **1994**, *37*, 907−912.
(36) Jones, M.; Rana, K. K.; Ward, J. G.; Young, R. C. Improved synthesis of inositol phospholipid analogues. *Tetrahedron Lett.* **1989**, *30*, 5353−5356.
(37) Mills, S. J.; Potter, B. V. L. Synthesis of the enantiomers of *myo*-inositol 1,2,4,5-tetrakisphosphate, a regioisomer of *myo*-inositol 1,3,4,5-tetrakisphosphate. *J. Chem. Soc., Perkin Trans. 1* **1997**, 1279−1286.
(38) Chiara, J. L.; Martín-Lomas, M. A Stereoselective route to enantiomerically pure *myo*-inositol derivatives starting from D-mannitol. *Tetrahedron Lett.* **1994**, *35*, 2969−2972.
(39) Rossi, A. M.; Riley, A. M.; Tovey, S. C.; Rahman, T.; Dellis, O.; Taylor, E. J.; Veresov, V. G.; Potter, B. V. L.; Taylor, C. W. Synthetic partial agonists reveal key steps in IP_3 receptor activation. *Nat. Chem. Biol.* **2009**, *5*, 631−639.
(40) Marchant, J. S.; Beecroft, M. D.; Riley, A. M.; Jenkins, D. J.; Marwood, R. D.; Taylor, C. W.; Potter, B. V. L. Disaccharide polyphosphates based upon adenophostin A activate hepatic D-*myo*-inositol 1,4,5-trisphosphate receptors. *Biochemistry* **1997**, *36*, 12780−12790.
(41) Shuto, S.; Horne, G.; Marwood, R. D.; Potter, B. V. L. Total synthesis of nucleobase-modified adenophostin A mimics. *Chem. - Eur. J.* **2001**, *7*, 4937−4946.
(42) Beecroft, M. D.; Marchant, J. S.; Riley, A. M.; van Straten, N. C. R.; Van der Marel, G. A.; van Boom, J. H.; Potter, B. V. L.; Taylor, C. W. Acyclophostin: a ribose-modified analog of adenophostin A with high affinity for inositol 1,4,5-trisphosphate receptors and pH-dependent efficacy. *Mol. Pharmacol.* **1999**, *55*, 109−117.
(43) Roussel, F.; Hilly, M.; Chrétien, F.; Manger, J.-P.; Chapleur, Y. Synthesis and biological evaluation of (2-hydroxyethyl)-2-deoxy-α-D-*threo*-pyranoside 3,4,2′-trisphosphate, a mimic of the second messenger inositol 1,4,5-trisphosphate. *J. Carbohydr. Chem.* **1999**, *18*, 697−707.
(44) Saleem, H.; Tovey, S. C.; Rahman, T.; Riley, A. M.; Potter, B. V. L.; Taylor, C. W. Stimulation of inositol 1,4,5-trisphosphate (IP_3) receptor subtypes by analogues of IP_3. *PLoS One* **2013**, *8*, No. e54877.
(45) Riley, A. M.; Correa, V.; Mahon, M. F.; Taylor, C. W.; Potter, B. V. L. Bicyclic analogs of D-*myo*-inositol 1,4,5-trisphosphate related to adenophostin A: synthesis and biological activity. *J. Med. Chem.* **2001**, *44*, 2108−2117.
(46) de Kort, M.; Regenbogen, A. D.; Valentijn, R. A. P. M.; Challiss, R. A. J.; Iwata, Y.; Miyamoto, S.; van der Marel, G. A.; van Boom, J. H. Spirophostins: conformationally restricted analogues of adenophostin A. *Chem. - Eur. J.* **2000**, *6*, 2696−2704.
(47) Parekh, A. B.; Fleig, A.; Penner, R. The store-operated calcium current I(CRAC): nonlinear activation by $InsP_3$ and dissociation from calcium release. *Cell* **1997**, *89*, 973−980.
(48) Parekh, A. B.; Riley, A. M.; Potter, B. V. L. Adenophostin A and ribophostin, but not inositol 1,4,5-trisphosphate or *manno*-adenophostin, activate the Ca^{2+} release-activated Ca^{2+} current, I_{CRAC}, in weak intracellular Ca^{2+} buffer. *Biochem. J.* **2002**, *361*, 133−141.

https://dx.doi.org/10.1021/acs.jmedchem.9b01986
J. Med. Chem. 2020, 63, 3238−3251